Supplementary Information for

Molecular features defining the efficiency of bioPROTACs

Dorothea Winkelvoß[§,1], David Vukovic[§,1], Anna-Carina Hänny[1], Luca Riermeier[1], Anto Udovcic[1], Jonas Kolibius[1], Annemarie Honegger[1], Peer R. E. Mittl[1], Erich Michel[1], Simon Hansen[1] and Andreas Plückthun[1,*]

[1] *Department of Biochemistry, University of Zurich, 8057 Zurich, Switzerland.*

[§] These authors contributed equally.

* Corresponding author:

Prof. Andreas Plückthun

Tel: +41 44 635 5570

Email: plueckthun@bioc.uzh.ch

Website: https://plueckthun.bioc.uzh.ch

Supplementary Figures

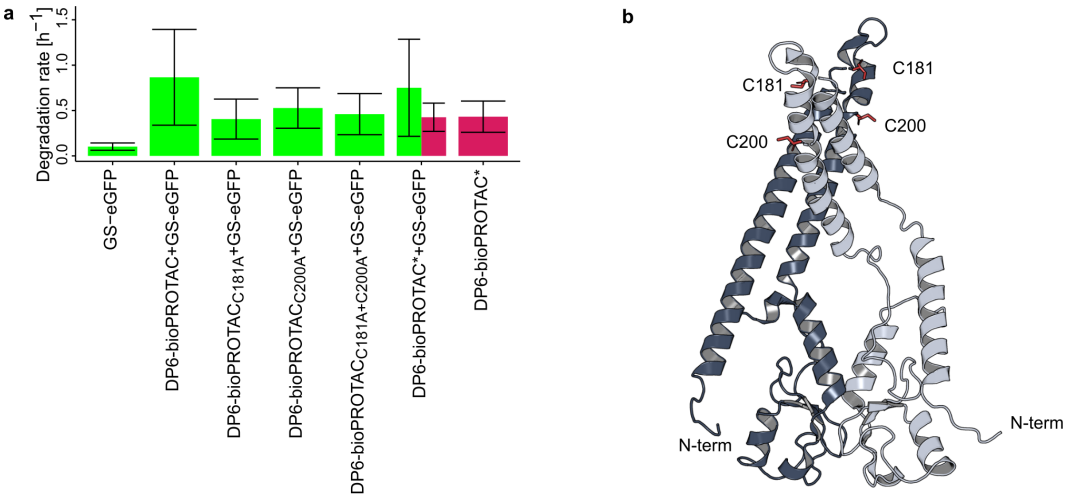

Supplementary Fig. S1. GS-eGFP degradation rates of DP6-bioPROTAC mutants where cysteines are substituted. a*, Average degradation rate constants of single cells as determined upon microinjection of 1-to-1 complexes into the cytosol of living cells, measured by fluorescent live-cell imaging. Error bars indicate standard deviations. Numbers of analyzed cells per analyte are shown in Supplementary Table ST2. GS-eGFP degradation rates are shown in green and degradation rates of bioPROTACs, labelled with TMR5-maleimide (indicated by an asterisk *) in the coiled coil regions, are shown in red. The CHIPΔTPR domain contains two surface-exposed cysteines that are available for labelling. Mutation of one or more surface exposed cysteines changes degradation rate, which is why the wt CHIPΔTPR domain was used for labelling.* ***b****, Structure of CHIP ligase dimer without TPR repeats (PDB ID: 2C2L). DARPins are genetically fused to the N-terminus. Surface-exposed cysteine residues used for maleimide-coupling of TMR5 dye are shown in red.*

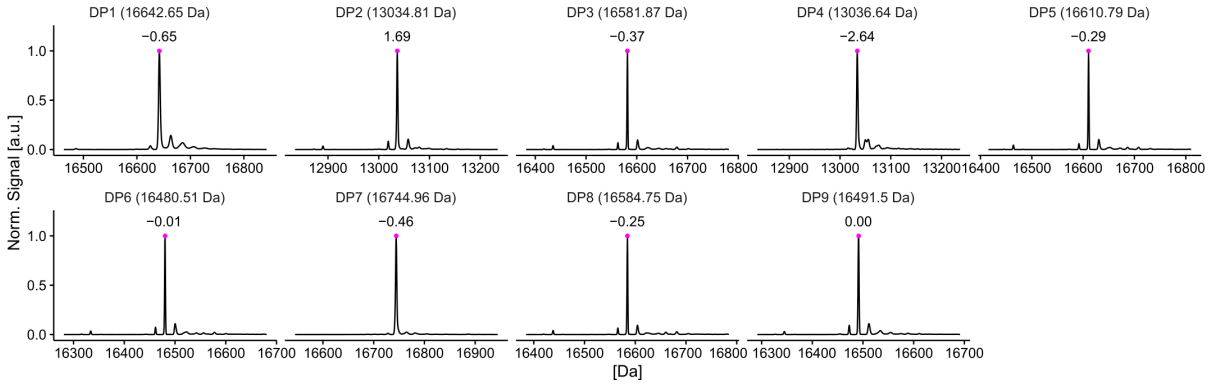

Supplementary Fig. S2. Quality control of purified DARPins. *Shown are electrospray ionization mass spectrometry (ESI-MS) spectra after deconvolution. Indicated are peaks with signals higher above baseline than 20% of the main peak. Values represent molecular mass differences between the expected mass after protein production.*

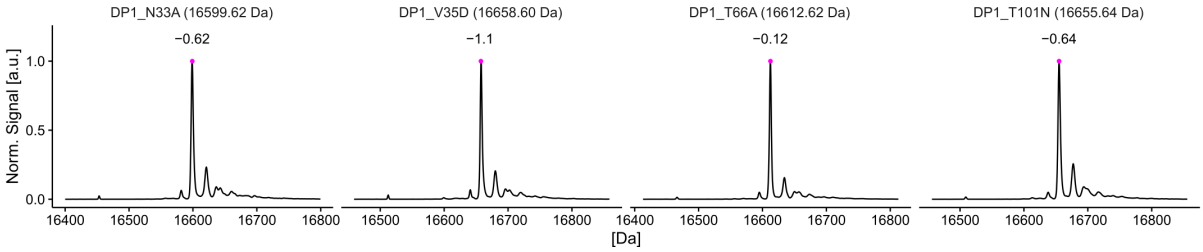

Supplementary Fig. S3. Quality control of purified derivatives of DARPin 1. *Shown are electrospray ionization mass spectrometry (ESI-MS) spectra after deconvolution. Indicated are peaks with signals higher above baseline than 20% of the main peak. Values represent molecular mass differences between the expected mass after protein production.*

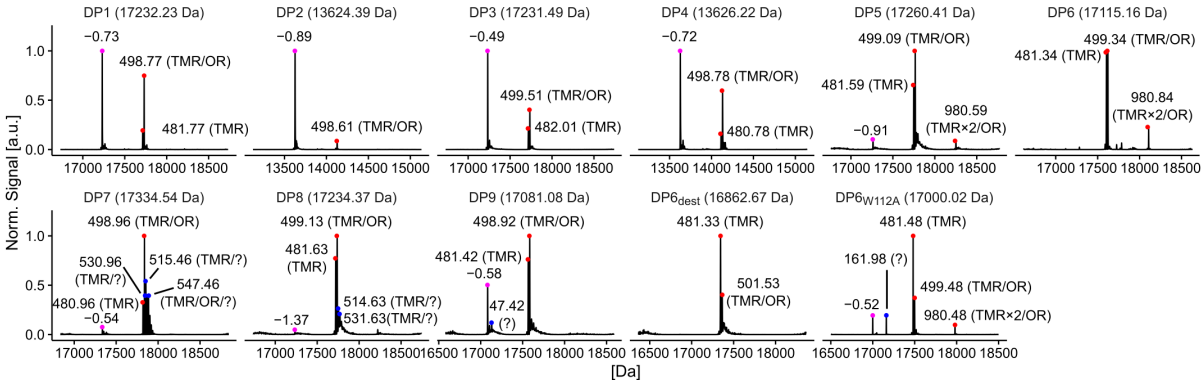

Supplementary Fig. S4. Quality control of purified and TMR-labeled DARPins. *Shown are electrospray ionization mass spectrometry (ESI-MS) spectra after deconvolution. Values represent molecular mass differences between uncoupled DARPin variants. Expected causes for indicated mass differences contain the addition of tetramethylrhodamine-5-maleimide (TMR, +481.51 Da). Maleimide-thiol conjugate stabilization by irreversible hydrolysis, structurally constituting an open ring (OR, +18.01 Da). Unexplained deviations encountered are labeled with a question mark.*

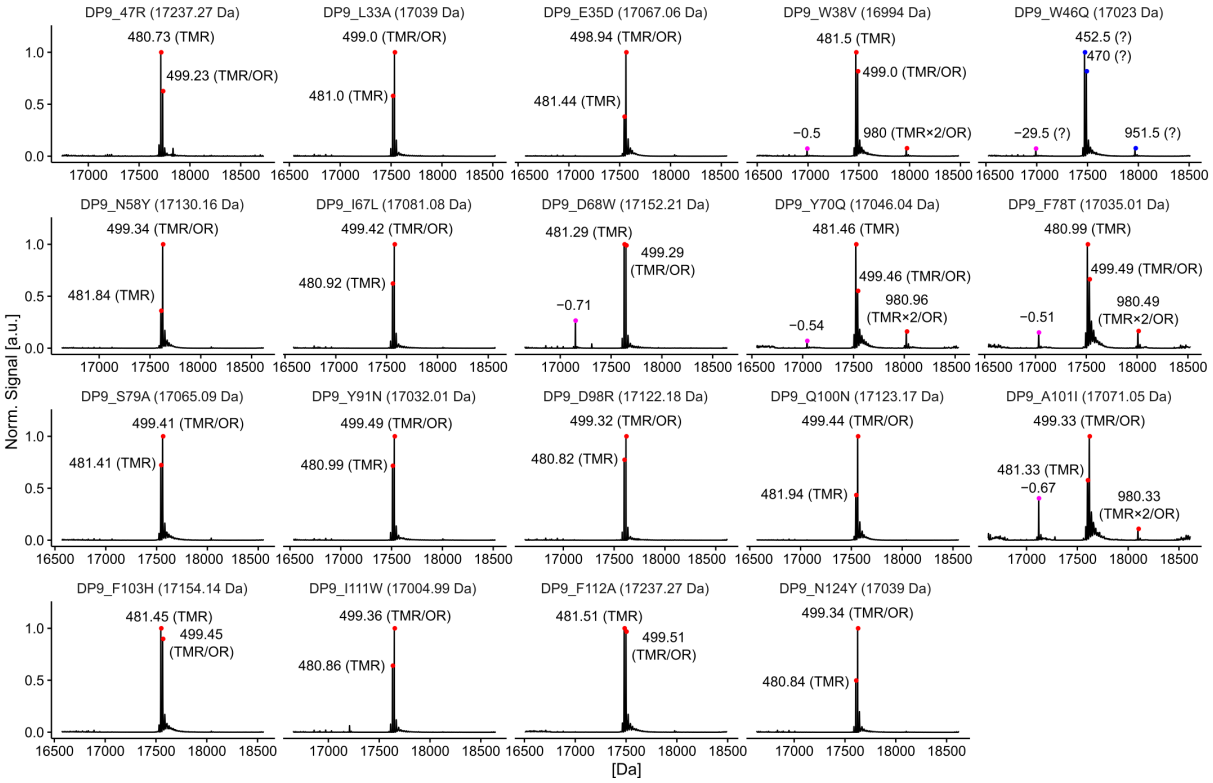

Supplementary Fig. S5. Quality control of purified and TMR-labeled DARPin 9 variants. *Shown are electrospray ionization mass spectrometry (ESI-MS) spectra after deconvolution. Values represent molecular mass differences between uncoupled DARPin variants. Expected causes for indicated mass differences contain the addition of tetramethylrhodamine-5-maleimide (TMR, +481.51 Da). Maleimide-thiol conjugate stabilization by irreversible hydrolysis, structurally constituting an open ring (OR, +18.01 Da). Unexplained deviations encountered are labeled with a question mark.*

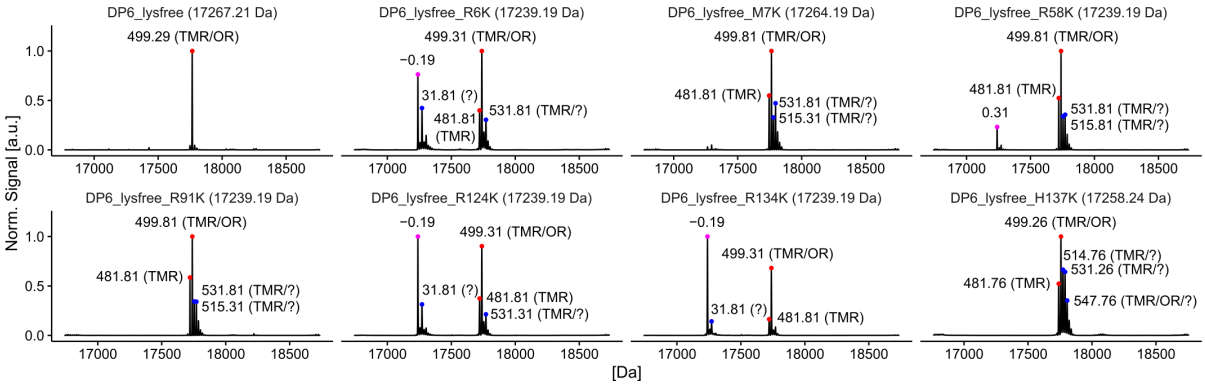

Supplementary Fig. S6. Quality control of purified and TMR-labeled single-lysine containing DARPin 6 variants. *Shown are electrospray ionization mass spectrometry (ESI-MS) spectra after deconvolution. Values represent molecular mass differences between uncoupled DARPin variants. Expected causes for indicated mass differences contain the addition of tetramethylrhodamine-5-maleimide (TMR, +481.51 Da). Maleimide-thiol conjugate stabilization by irreversible hydrolysis, structurally constituting an open ring (OR, +18.01 Da). Unexplained deviations encountered are labeled with a question mark.*

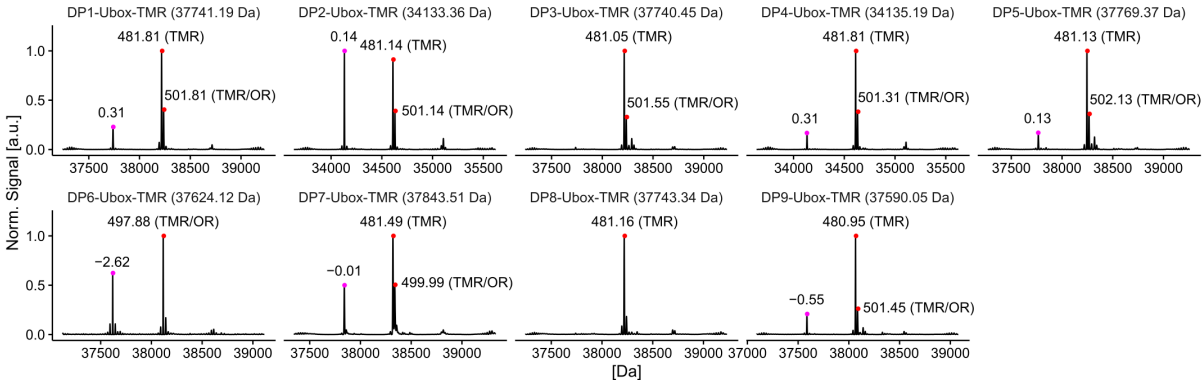

Supplementary Fig. S7. Quality control of purified and TMR-labeled bioPROTACs. *The CHIPΔTPR domain is denoted "Ubox". Shown are electrospray ionization mass spectrometry (ESI-MS) spectra after deconvolution. Values represent molecular mass differences between uncoupled DARPin variants. Expected causes for indicated mass differences contain the addition of tetramethylrhodamine-5-maleimide (TMR, +481.51 Da). Maleimide-thiol conjugate stabilization by irreversible hydrolysis, structurally constituting an open ring (OR, +18.01 Da).*

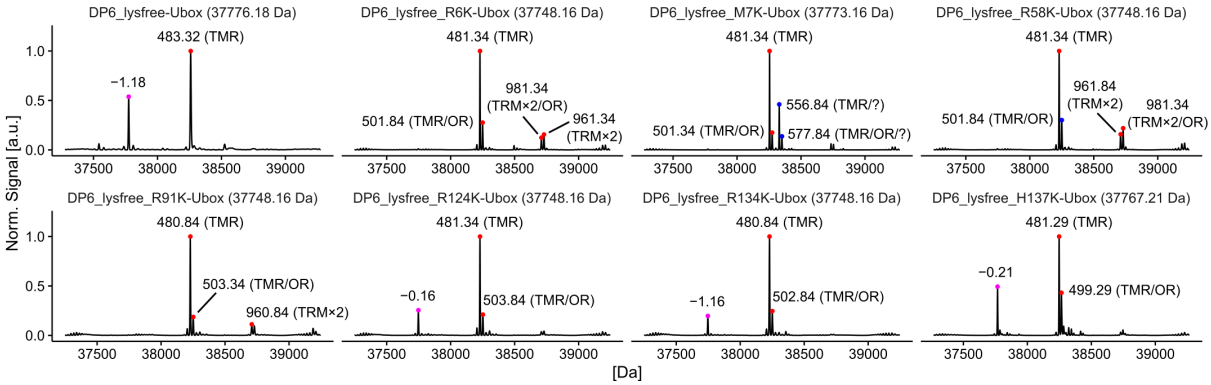

Supplementary Fig. S8. Quality control of purified and TMR-labeled bioPROTACs, based on single-lysine containing DARPin 6 derivatives. *The CHIPΔTPR domain is denoted "Ubox". Shown are electrospray ionization mass spectrometry (ESI-MS) spectra after deconvolution. Values represent molecular mass differences between uncoupled DARPin variants. Expected causes for indicated mass differences contain the addition of tetramethylrhodamine-5-maleimide (TMR, +481.51 Da). Maleimide-thiol conjugate stabilization by irreversible hydrolysis, structurally constituting an open ring (OR, +18.01 Da).*

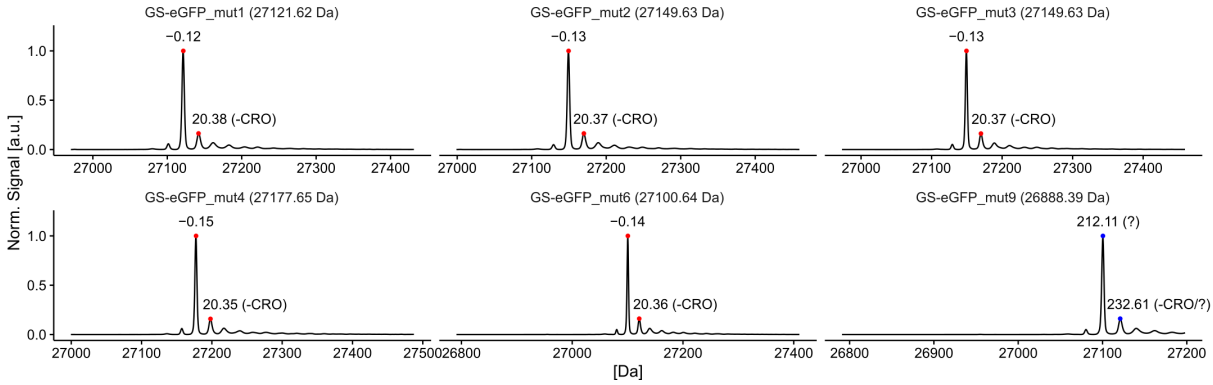

Supplementary Fig. S9. Quality control of purified GS-eGFP derivatives. *Shown are electrospray ionization mass spectrometry (ESI-MS) spectra after deconvolution. Values represent molecular mass differences between uncoupled DARPin variants. Expected causes for indicated mass differences contain the unformed chromophore (-CRO, +20.01527). Unexplained deviations are labeled with a question mark.*

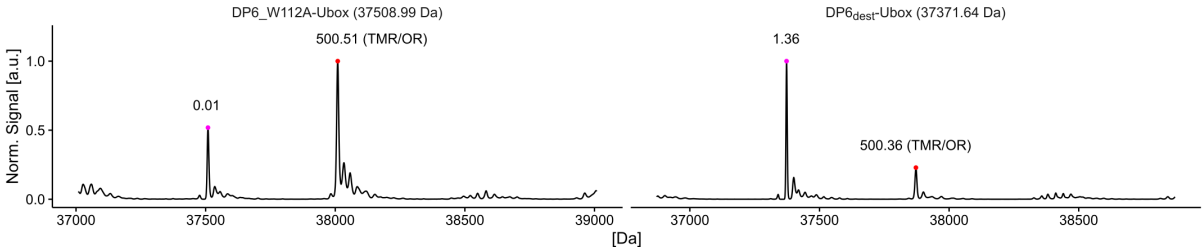

Supplementary Fig. S10. Quality control of purified and TMR-labeled bioPROTACs, based on DARPin 6 derivatives. *The CHIPΔTPR domain is denoted "Ubox". Shown are electrospray ionization mass spectrometry (ESI-MS) spectra after deconvolution. Values represent molecular mass differences between uncoupled DARPin variants. Expected causes for indicated mass differences contain the addition of tetramethylrhodamine-5-maleimide (TMR, +481.51 Da). Maleimide-thiol conjugate stabilization by irreversible hydrolysis, structurally constituting an open ring (OR, +18.01 Da).*

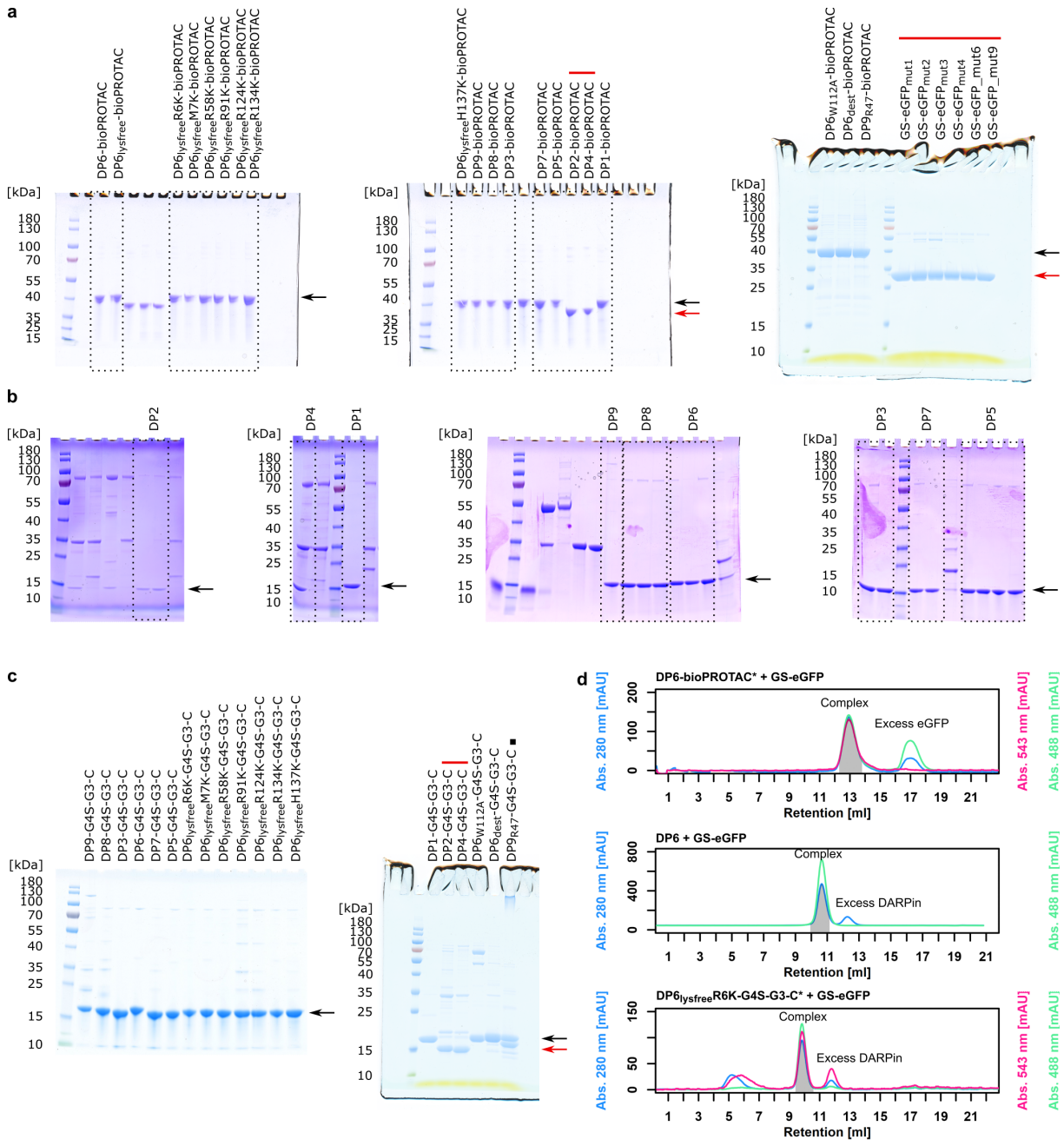
a
DP6-bioPROTAC
DP6lysfree-bioPROTAC
DP6lysfreeR6K-bioPROTAC
DP6lysfreeM7K-bioPROTAC
DP6lysfreeR58K-bioPROTAC
DP6lysfreeR91K-bioPROTAC
DP6lysfreeR124K-bioPROTAC
DP6lysfreeR134K-bioPROTAC
DP6lysfreeH137K-bioPROTAC
DP9-bioPROTAC
DP8-bioPROTAC
DP3-bioPROTAC
DP7-bioPROTAC
DP5-bioPROTAC
DP2-bioPROTAC
DP4-bioPROTAC
DP1-bioPROTAC
DP6W112A-bioPROTAC
DP6dest-bioPROTAC
DP9R47-bioPROTAC
GS-eGFPmut1
GS-eGFPmut2
GS-eGFPmut3
GS-eGFPmut4
GS-eGFP_mut6
GS-eGFP_mut9
[kDa]
180
130
100
70
55
40
35
25
15
10
b
DP2
DP4
DP1
DP9
DP8
DP6
DP3
DP7
DP5
c
DP9-G4S-G3-C
DP8-G4S-G3-C
DP3-G4S-G3-C
DP6-G4S-G3-C
DP7-G4S-G3-C
DP5-G4S-G3-C
DP6lysfreeR6K-G4S-G3-C
DP6lysfreeM7K-G4S-G3-C
DP6lysfreeR58K-G4S-G3-C
DP6lysfreeR91K-G4S-G3-C
DP6lysfreeR124K-G4S-G3-C
DP6lysfreeR134K-G4S-G3-C
DP6lysfreeH137K-G4S-G3-C
DP1-G4S-G3-C
DP2-G4S-G3-C
DP4-G4S-G3-C
DP6W112A-G4S-G3-C
DP6dest-G4S-G3-C
DP9R47-G4S-G3-C
d
DP6-bioPROTAC* + GS-eGFP
Complex
Excess eGFP
Abs. 280 nm [mAU]
Abs. 543 nm [mAU]
Abs. 488 nm [mAU]
Retention [ml]
DP6 + GS-eGFP
Excess DARPin
DP6lysfreeR6K-G4S-G3-C* + GS-eGFP

Supplementary Fig. S11. Quality control of purified proteins by SDS-PAGE and eGFP complexation by SEC. *SDS-PAGE was performed after IMAC and AEX purification. Prior to microinjection into live cells, samples underwent further purification by SEC or, after fluorescent labeling, by AEX and SEC. a, SDS-PAGE gels of DP-bioPROTAC constructs (~37 kDa, except for N2C DARPin constructs with DP2 and DP4, marked in red, ~34 kDa) and GS-eGFP mutants (~27 kDa). b, SDS-PAGE gels of DARPin constructs (~16 kDa, except for N2C DARPins DP2 and DP4, ~13 kDa). c, SDS-PAGE gels of single-cysteine DARPin constructs for fluorescent labeling (~17 kDa, except for N2C DARPins DP2 and DP4, marked in red, ~14 kDa). Black square (■): The presence of two bands is characteristic of highly stable DARPins which do not fully denature in SDS-PAGE. d, Representative chromatograms of eGFP complex purification by SEC. DARPin or bioPROTAC-dimer samples were mixed with eGFP in a ratio ensuring a 1:1 complex after purification. Collected fractions are indicated in grey. Labelled species is indicated by *. Absorbance at 280 nm (protein) is shown in blue, at 488 nm (eGFP and minimal TMR-dye signal) in green, and at 543 nm (TMR-dye) in pink. Upper panel: Superdex 200. Middle and bottom panels: Superdex 75.*

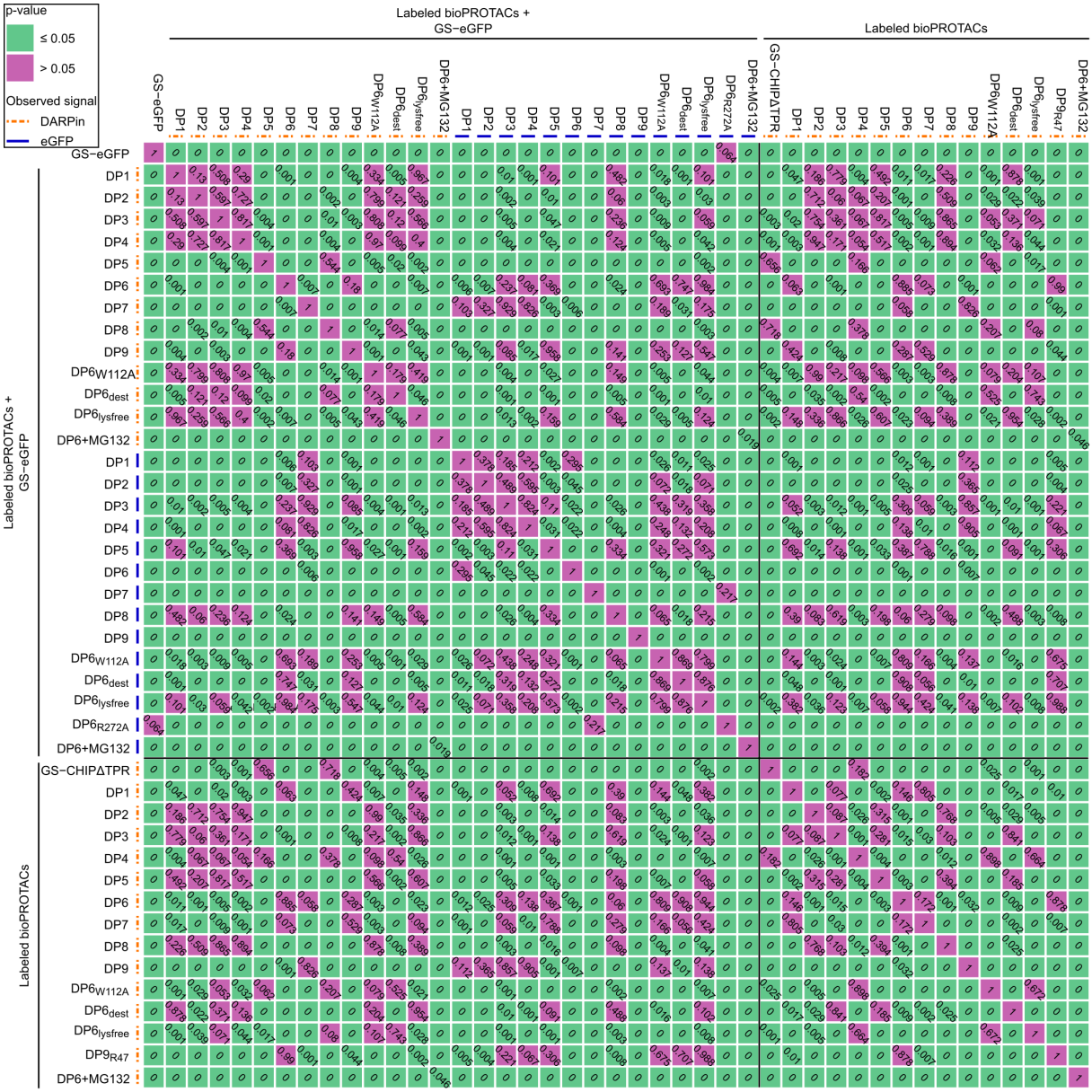

Supplementary Fig. S12. Assessment of statistical significance of degradation rate differences of DARPin-based bioPROTACs and bioPROTAC/GS-eGFP complexes from Fig. 2a and b. *P-values were calculated using an unpaired Student's t-test (two-sided), comparing averaged degradation rate constants obtained from individual cells injected with the analytes in question. Green tiles indicate a high likelihood of statistically significant rate differences. "0" is a shorthand for < 0.001.*

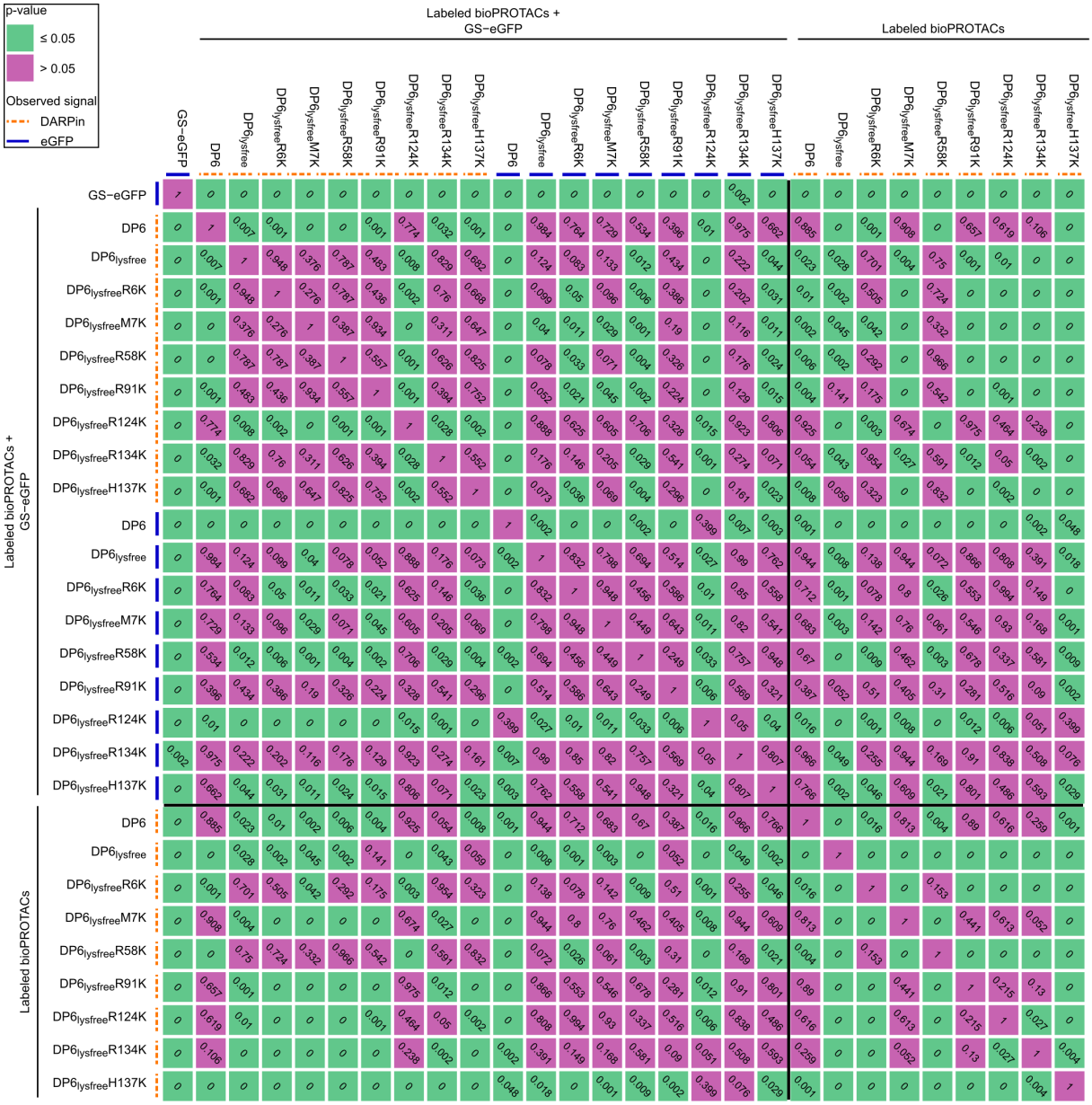

Supplementary Fig. S13. Assessment of statistical significance of degradation rate differences of DARPin-based bioPROTACs and bioPROTAC/GS-eGFP complexes from Supplementary Fig. S26a and b. *P-values were calculated using an unpaired Student's t-test (two-sided), comparing averaged degradation rate constants obtained from individual cells injected with the analytes in question. Green tiles indicate a high likelihood of statistically significant rate differences. "0" is a shorthand for < 0.001.*

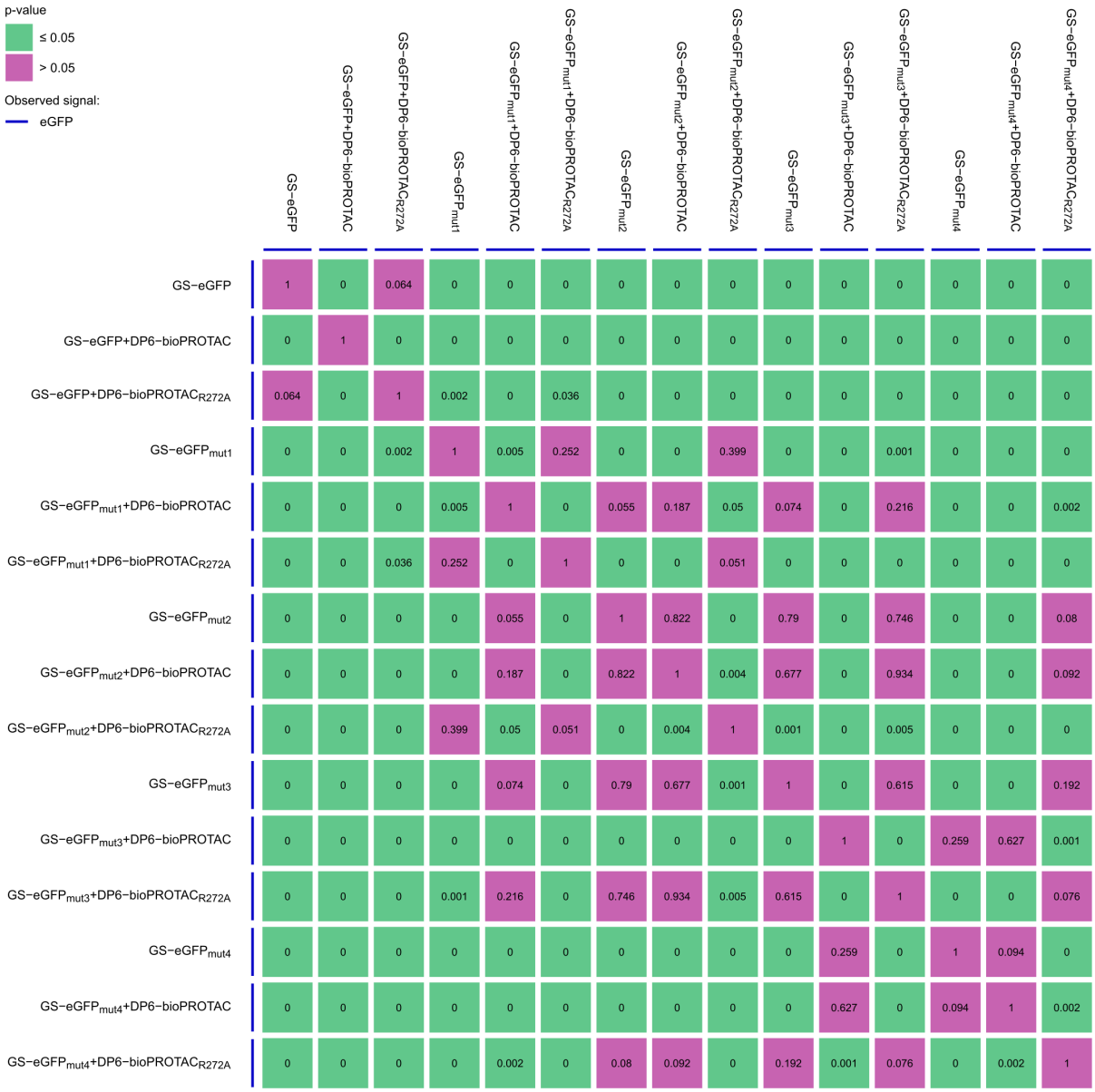

	GS−eGFP	GS−eGFP+DP6−bioPROTAC	GS−eGFP+DP6−bioPROTAC$_{R272A}$	GS−eGFP$_{mut1}$	GS−eGFP$_{mut1}$+DP6−bioPROTAC	GS−eGFP$_{mut1}$+DP6−bioPROTAC$_{R272A}$	GS−eGFP$_{mut2}$	GS−eGFP$_{mut2}$+DP6−bioPROTAC	GS−eGFP$_{mut2}$+DP6−bioPROTAC$_{R272A}$	GS−eGFP$_{mut3}$	GS−eGFP$_{mut3}$+DP6−bioPROTAC	GS−eGFP$_{mut3}$+DP6−bioPROTAC$_{R272A}$	GS−eGFP$_{mut4}$	GS−eGFP$_{mut4}$+DP6−bioPROTAC	GS−eGFP$_{mut4}$+DP6−bioPROTAC$_{R272A}$
GS−eGFP	1	0	0.064	0	0	0	0	0	0	0	0	0	0	0	0
GS−eGFP+DP6−bioPROTAC	0	1	0	0	0	0	0	0	0	0	0	0	0	0	0
GS−eGFP+DP6−bioPROTAC$_{R272A}$	0.064	0	1	0.002	0	0.036	0	0	0	0	0	0	0	0	0
GS−eGFP$_{mut1}$	0	0	0.002	1	0.005	0.252	0	0	0.399	0	0	0.001	0	0	0
GS−eGFP$_{mut1}$+DP6−bioPROTAC	0	0	0	0.005	1	0	0.055	0.187	0.05	0.074	0	0.216	0	0	0.002
GS−eGFP$_{mut1}$+DP6−bioPROTAC$_{R272A}$	0	0	0.036	0.252	0	1	0	0	0.051	0	0	0	0	0	0
GS−eGFP$_{mut2}$	0	0	0	0	0.055	0	1	0.822	0	0.79	0	0.746	0	0	0.08
GS−eGFP$_{mut2}$+DP6−bioPROTAC	0	0	0	0	0.187	0	0.822	1	0.004	0.677	0	0.934	0	0	0.092
GS−eGFP$_{mut2}$+DP6−bioPROTAC$_{R272A}$	0	0	0	0.399	0.05	0.051	0	0.004	1	0.001	0	0.005	0	0	0
GS−eGFP$_{mut3}$	0	0	0	0	0.074	0	0.79	0.677	0.001	1	0	0.615	0	0	0.192
GS−eGFP$_{mut3}$+DP6−bioPROTAC	0	0	0	0	0	0	0	0	0	0	1	0	0.259	0.627	0.001
GS−eGFP$_{mut3}$+DP6−bioPROTAC$_{R272A}$	0	0	0	0.001	0.216	0	0.746	0.934	0.005	0.615	0	1	0	0	0.076
GS−eGFP$_{mut4}$	0	0	0	0	0	0	0	0	0	0	0.259	0	1	0.094	0
GS−eGFP$_{mut4}$+DP6−bioPROTAC	0	0	0	0	0	0	0	0	0	0	0.627	0	0.094	1	0.002
GS−eGFP$_{mut4}$+DP6−bioPROTAC$_{R272A}$	0	0	0	0	0.002	0	0.08	0.092	0	0.192	0.001	0.076	0	0.002	1

Supplementary Fig. S14. Assessment of statistical significance of degradation rate differences of GS-eGFP mutants with DP6-based bioPROTACs from Fig. 3d. *P-values were calculated using an unpaired Student's t-test (two-sided), comparing averaged degradation rate constants obtained from individual cells injected with the analytes in question. Green tiles indicate a high likelihood of statistically significant rate differences. "0" is a shorthand for < 0.001.*

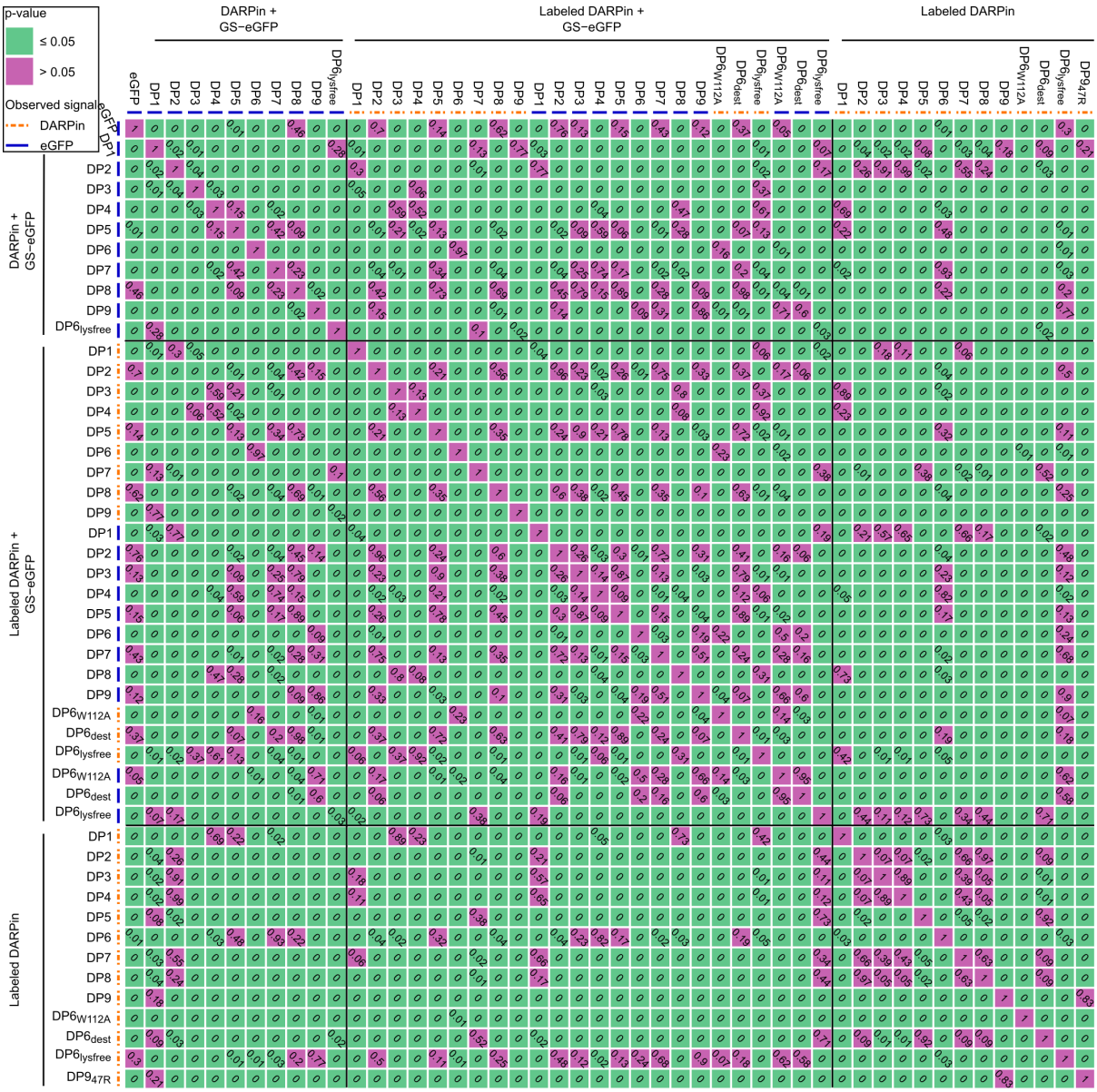

Supplementary Fig. S15. Assessment of statistical significance of degradation rate differences of DARPins and DARPin/GS-eGFP complexes from Fig. 4a-c. *P-values were calculated using an unpaired Student's t-test (two-sided), comparing averaged degradation rate constants obtained from individual cells injected with the analytes in question. Green tiles indicate a high likelihood of statistically significant rate differences. "0" is a shorthand for < 0.001.*

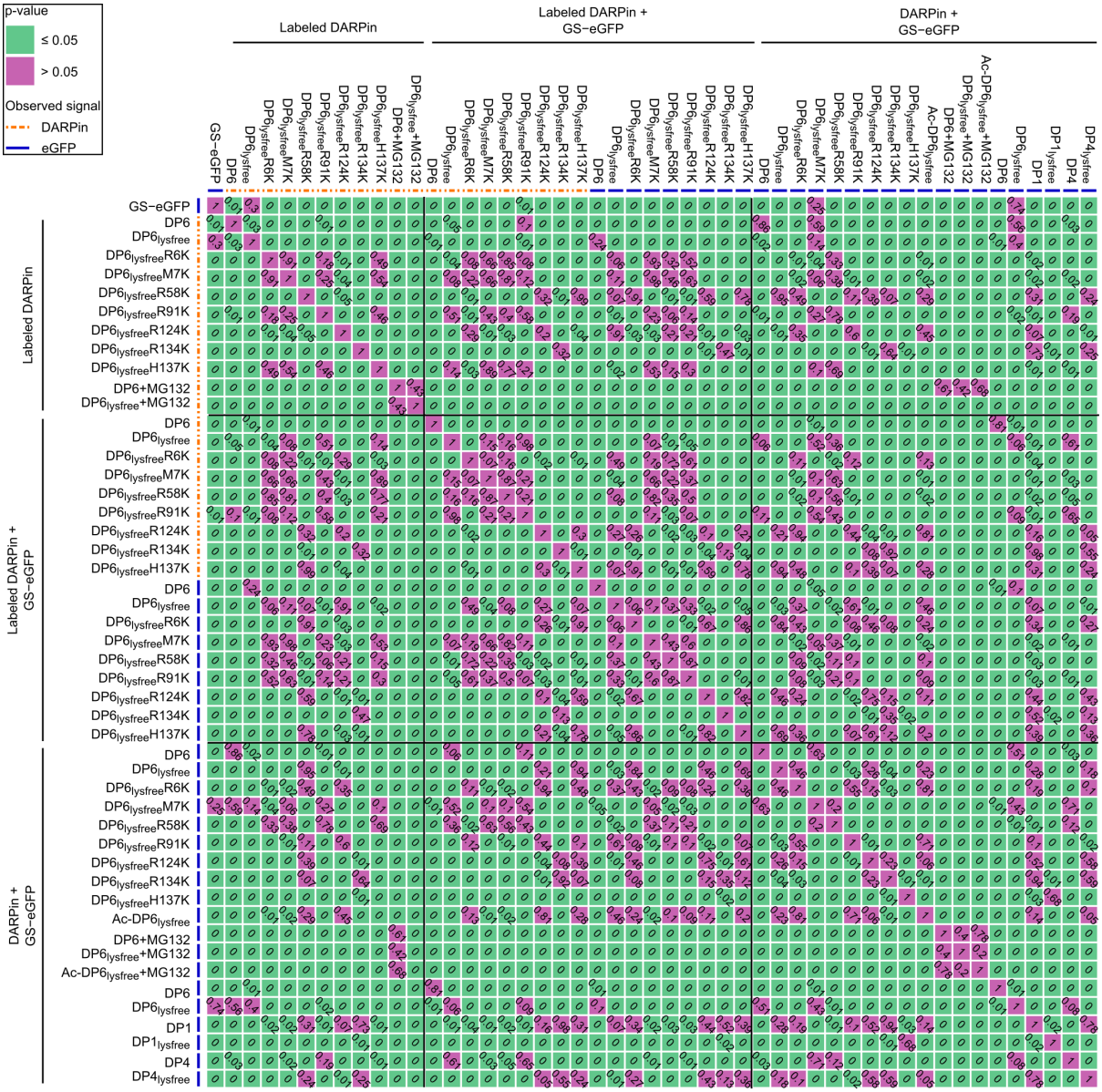

Supplementary Fig. S16. Assessment of statistical significance of degradation rate differences of DARPins and DARPin/GS-eGFP complexes from Fig. 4k-o. *P-values were calculated using an unpaired Student's t-test (two-sided), comparing averaged degradation rate constants obtained from individual cells injected with the analytes in question. Green tiles indicate a high likelihood of statistically significant rate differences. "0" is a shorthand for < 0.001.*

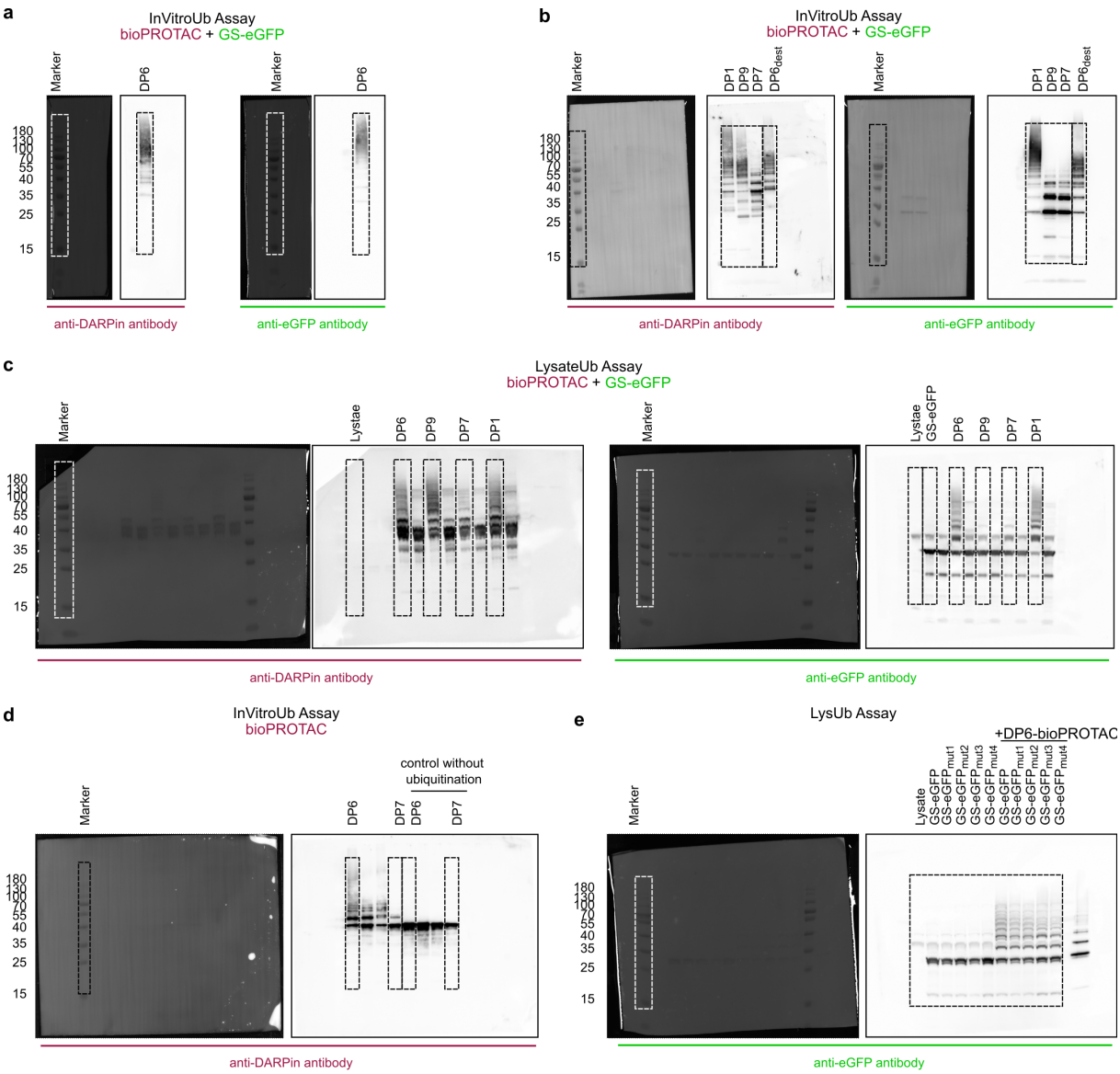
a
InVitroUb Assay
bioPROTAC + GS-eGFP
Marker
DP6
Marker
DP6
180
130
100
70
55
40
35
25
15
anti-DARPin antibody
anti-eGFP antibody
b
InVitroUb Assay
bioPROTAC + GS-eGFP
Marker
DP1
DP9
DP7
DP6dest
Marker
DP1
DP9
DP7
DP6dest
180
130
100
70
55
40
35
25
15
anti-DARPin antibody
anti-eGFP antibody
c
LysateUb Assay
bioPROTAC + GS-eGFP
Marker
Lystae
DP6
DP9
DP7
DP1
Marker
Lystae
GS-eGFP
DP6
DP9
DP7
DP1
180
130
100
70
55
40
35
25
15
anti-DARPin antibody
anti-eGFP antibody
d
InVitroUb Assay
bioPROTAC
Marker
control without ubiquitination
DP6
DP7
DP6
DP7
180
130
100
70
55
40
35
25
15
anti-DARPin antibody
e
LysUb Assay
+DP6-bioPROTAC
Marker
Lysate
GS-eGFP
GS-eGFPmut1
GS-eGFPmut2
GS-eGFPmut3
GS-eGFPmut4
GS-eGFP
GS-eGFPmut1
GS-eGFPmut2
GS-eGFPmut3
GS-eGFPmut4
180
130
100
70
55
40
35
25
15
anti-eGFP antibody

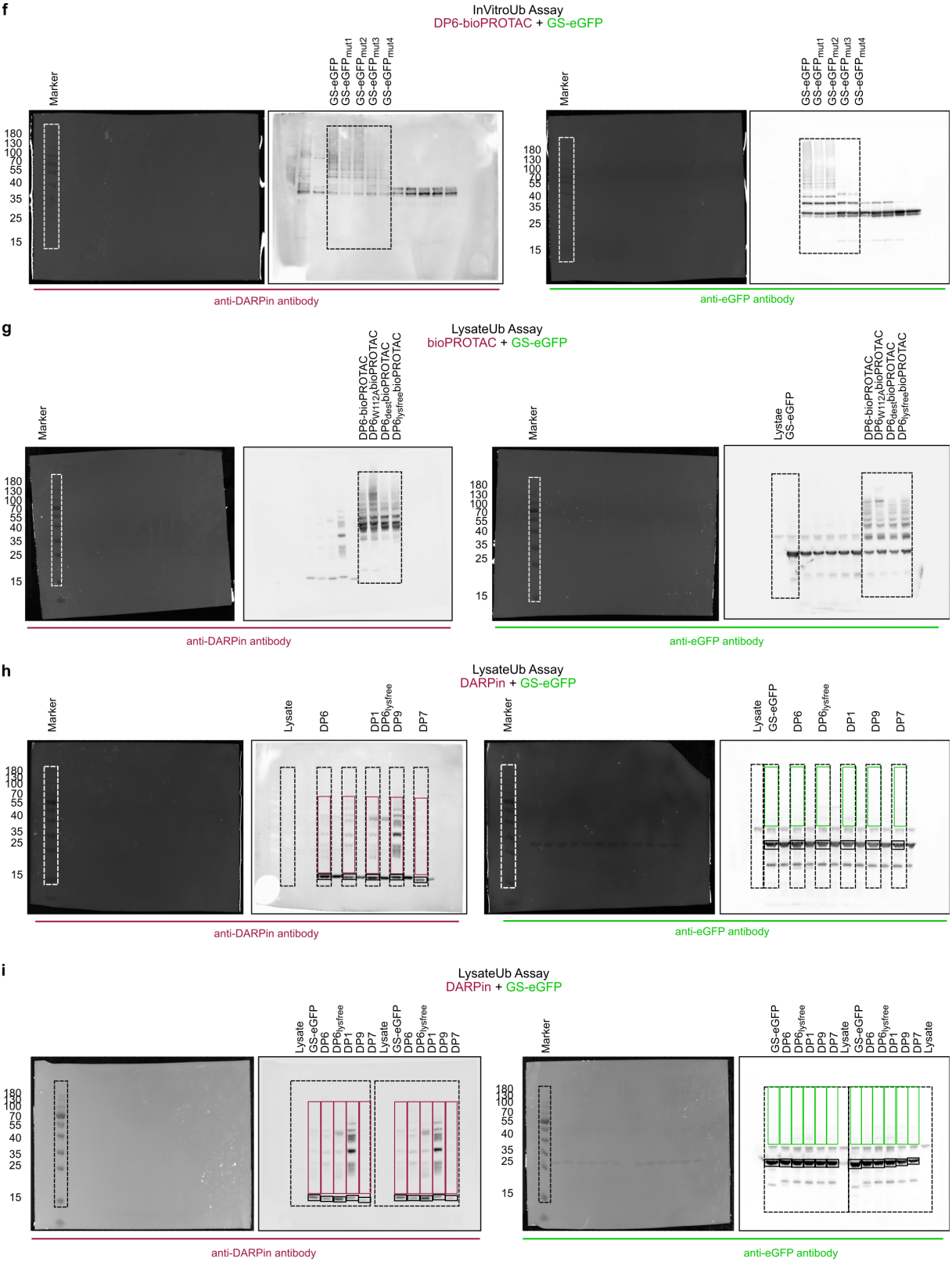
f
InVitroUb Assay
DP6-bioPROTAC + GS-eGFP
Marker
GS-eGFP
GS-eGFPmut1
GS-eGFPmut2
GS-eGFPmut3
GS-eGFPmut4
180
130
100
70
55
40
35
25
15
anti-DARPin antibody
anti-eGFP antibody
g
LysateUb Assay
bioPROTAC + GS-eGFP
DP6-bioPROTAC
DP6W112ABioPROTAC
DP6desBioPROTAC
DP6lysfreeBioPROTAC
Lysate
GS-eGFP
anti-DARPin antibody
anti-eGFP antibody
h
LysateUb Assay
DARPin + GS-eGFP
Lysate
DP6
DP1
DP6lysfree
DP9
DP7
anti-DARPin antibody
anti-eGFP antibody
i
LysateUb Assay
DARPin + GS-eGFP
anti-DARPin antibody
anti-eGFP antibody

Supplementary Fig. S17. Raw data of western blots. *Shown is the same membrane, imaged in the marker channel (left picture) and in the chemiluminescent channel to image the HRP substrate signal (right picture). Cropped areas used in figures are shown with a dashed line.* ***a****, DP6 lanes of Fig. 2h.* ***b****, Other lanes of Fig. 2h and* $DP6_{dest}$ *lanes of Supplementary Fig. S22b.* ***c****, Fig. 2g.* ***d****, Fig. 2i.* ***e****, Fig. 3e.* ***f****, Fig. 3c.* ***g****, Supplementary Fig. S22a.* ***h****, Fig. 4h.* ***i****, Supplementary Fig. S35.* ***h-i****, areas used for quantification of eGFP ubiquitination (green squares) and DARPin ubiquitination (magenta squares) and areas used for normalized to either unmodified eGFP or DARPin (black squares). Blots shown in a-g were recorded from single experiments and h-i show biological triplicates used for quantification.*

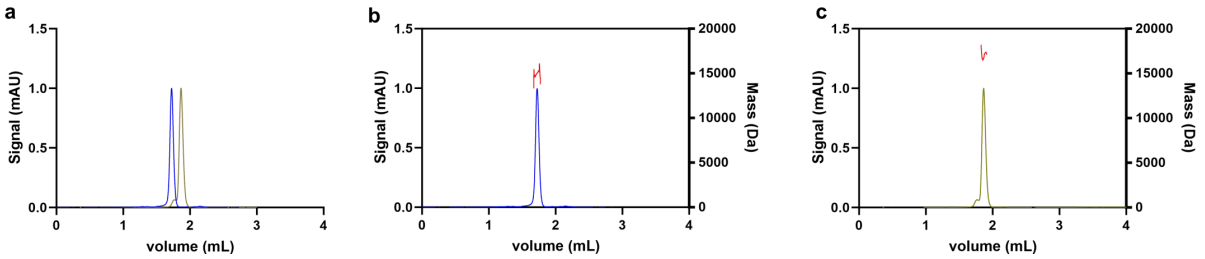

***Supplementary Fig. S18. SEC-MALS measurements of DP6 and DP7. a**, SEC profile of DP6 (blue) and DP7 (gold). Although they have the same mass, DP7 elutes later than DP6, indicating interaction with the column material. **b**, Mass profile of DP6 (red line) determined by SEC-MALS. **c**, Mass profile of DP7 (red line) determined by SEC-MALS. The scale on the right indicates the mass determined by MALS, indicating that both DP6 and DP7 have the expected molecular mass of a monomeric DARPin.*

DP1

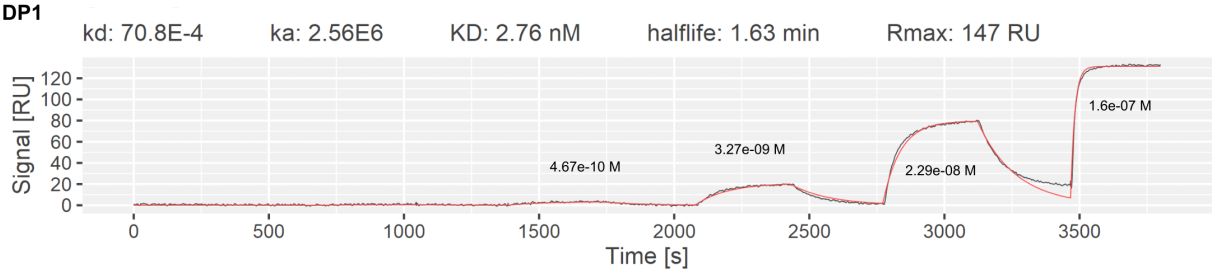

DP2

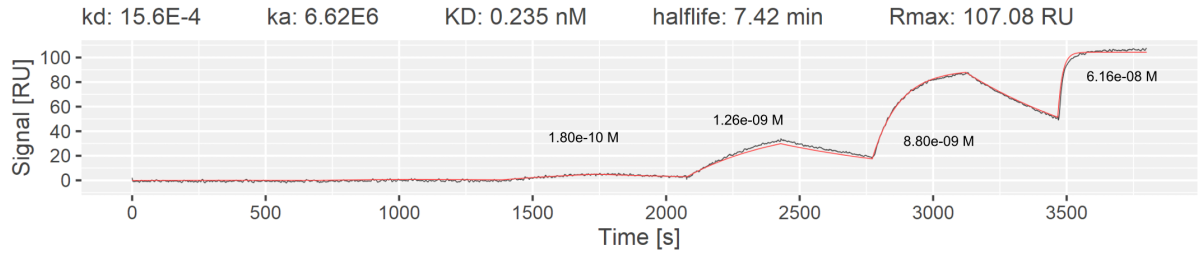

DP3

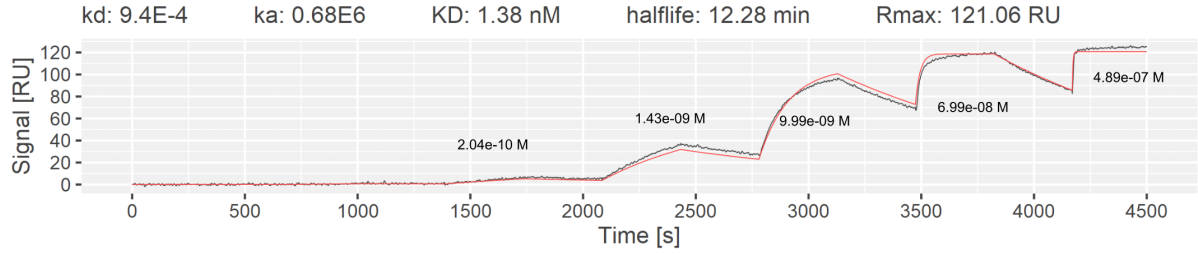

DP4

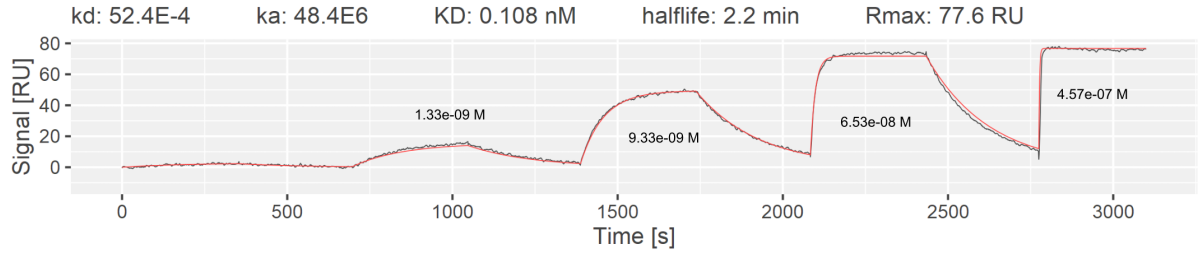

DP5

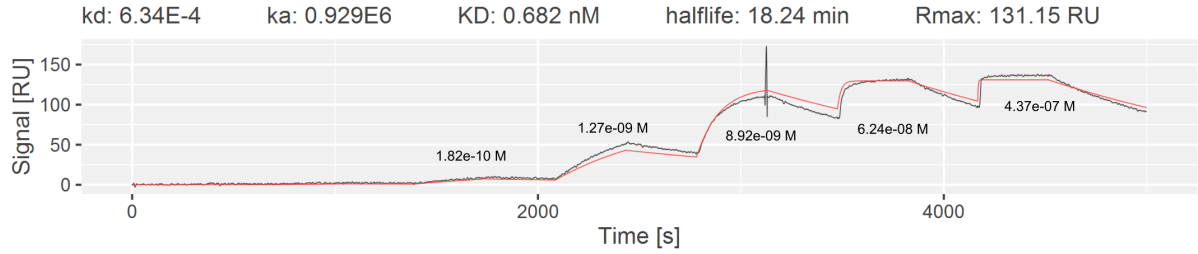

DP6

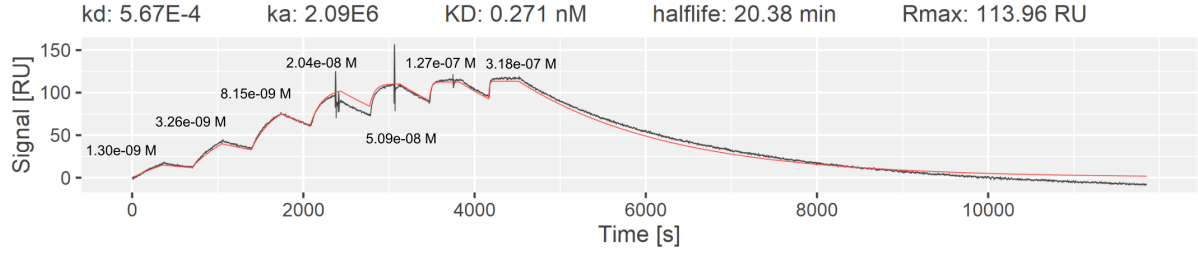

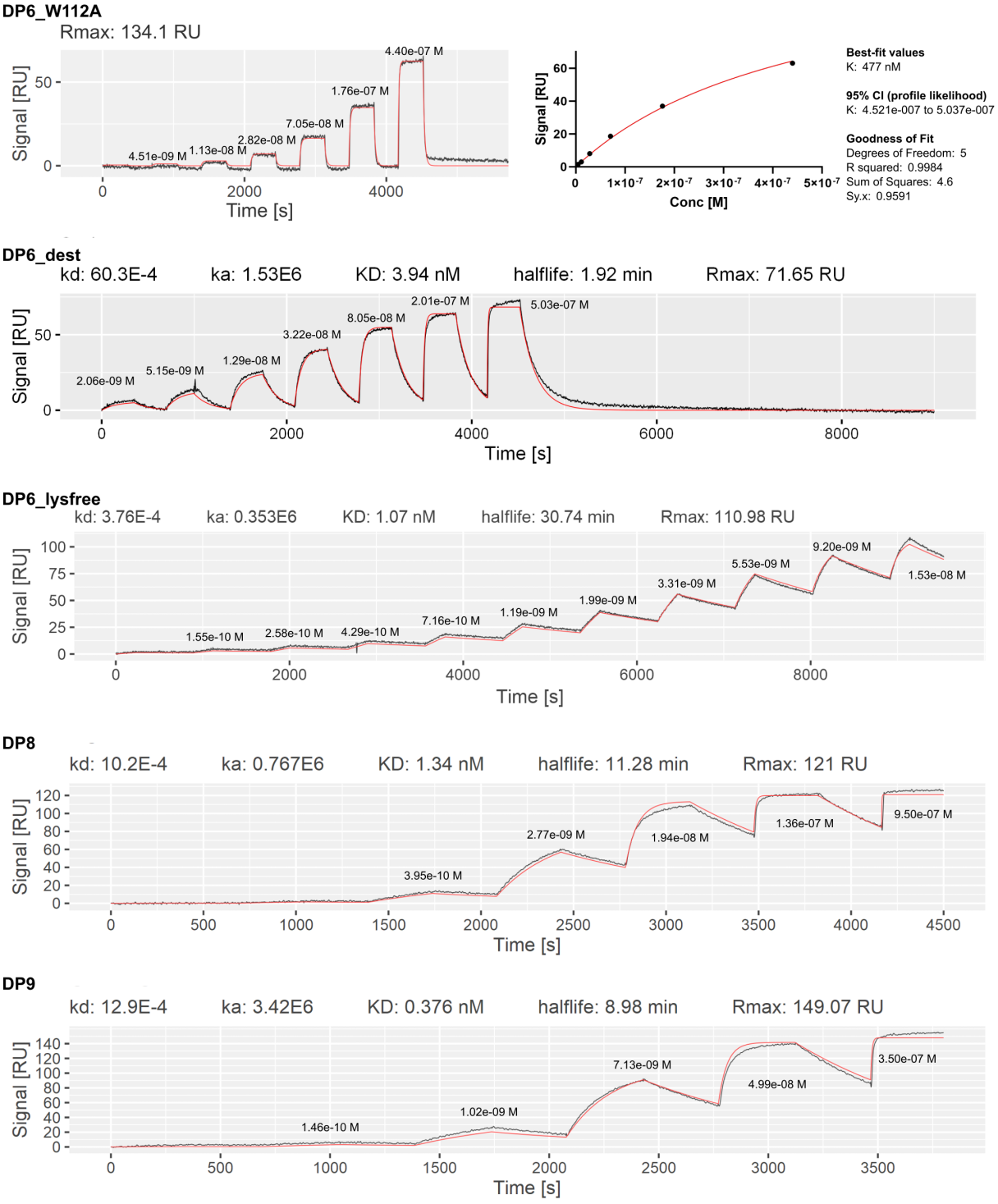

Supplementary Fig. S19. Surface plasmon resonance sensograms of eGFP-binding DARPins. *Biotinylated GS-eGFP was immobilized on a streptavidin chip. Kinetic titration experiments were performed. The experimental traces are shown in black, and the global fit is shown in red. $DP6_{W112}$ was fit globally to retrieve R_{max} and then K_D was determined by equilibrium analysis of the plateaus at the injected concentrations.*

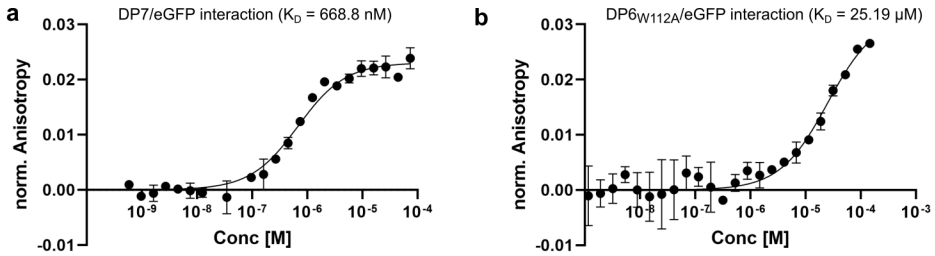

Supplementary Fig. S20. K_D determination of eGFP-binding DARPins by fluorescence anisotropy. *GS-eGFP at 20 nM was constant and the indicated DARPin was titrated. Shown are data from two technical replicates. Error bars represent the standard deviation.*

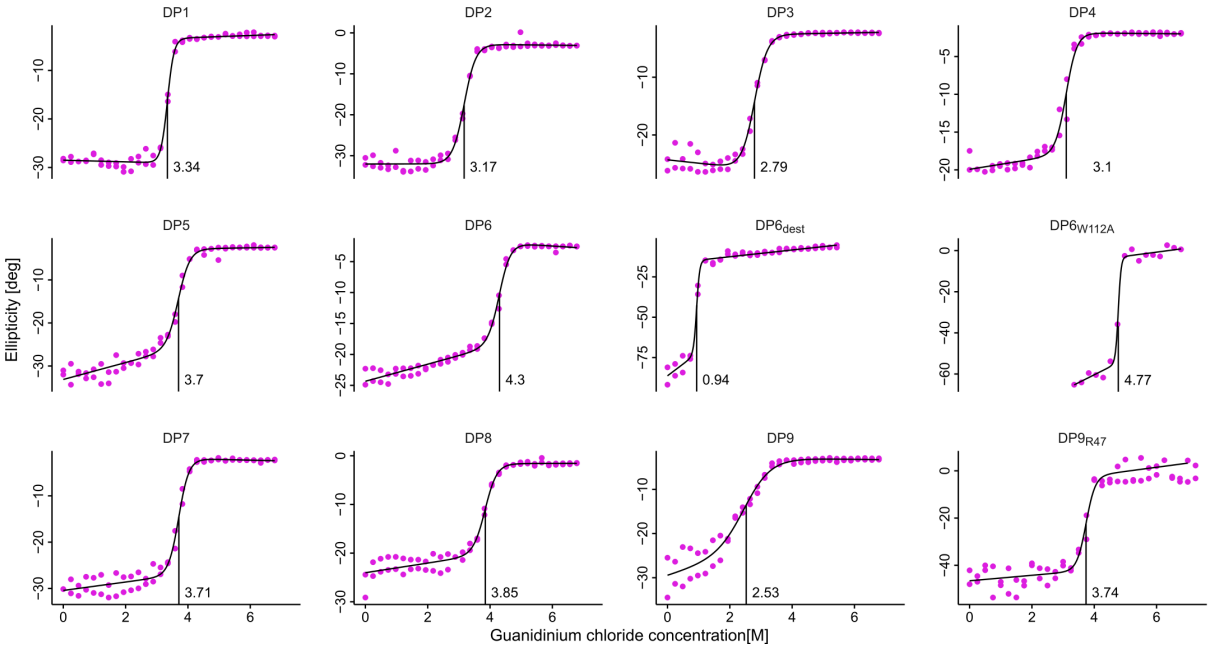

Supplementary Fig. S21. DARPin equilibrium unfolding as a function of guanidinium chloride concentration, observed using circular dichroism spectrometry. *For DP6, a mutant with Y59C was used here but the stability is expected to be similar, especially given the comparable unfolding midpoint of DP6$_{W112A}$.*

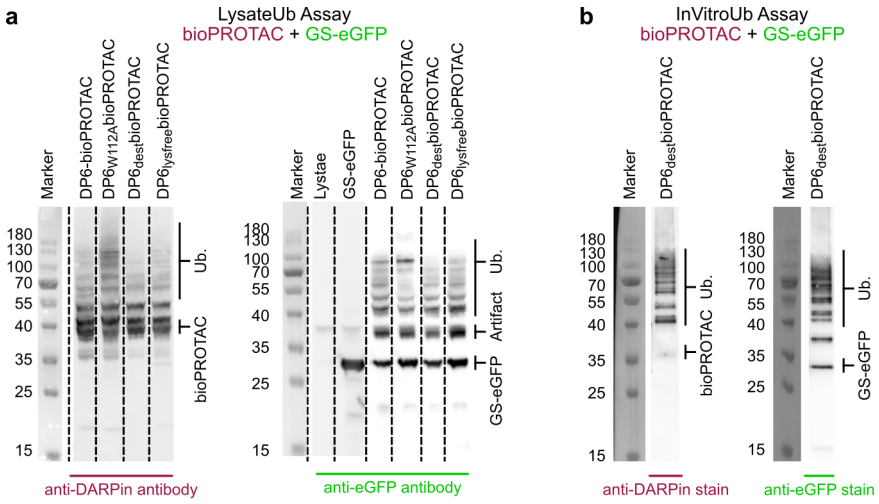

Supplementary Fig. S22. Ubiquitination assays of DP6-bioPROTAC mutants in complex with GS-eGFP. ***a****, Western blot images of LysateUb assay of GS-eGFP/DP6-bioPROTAC, GS-eGFP/DP6$_{W112A}$-bioPROTAC, GS-eGFP/DP6$_{dest}$-bioPROTAC and GS-eGFP/DP6$_{lysfree}$-bioPROTAC complexes. Samples were split for staining with anti-eGFP antibody or anti-DARPin serum to detect GS-eGFP or bioPROTAC ubiquitination.* **To image marker bands and antibody-stained bands, membranes were imaged in two separate channels. Uncropped membranes are shown in Supplementary Fig. S17.** *The mutant W112A strongly reduces eGFP binding affinity. The mutant DP6$_{dest}$ contains Leu to Ala mutations at L8 and L24 in every internal repeat (relative numbering in each repeat) to reduce its structural stability.* ***b****, Western blot images of CHIP/bioPROTAC InVitroUb assay of DP6$_{dest}$-bioPROTAC construct. Samples were split for staining with anti-eGFP antibody or anti DARPin serum to detect GS-eGFP or bioPROTAC ubiquitination. Unedited blots can be seen in Fig. S16. Shown are data from single experiments.*

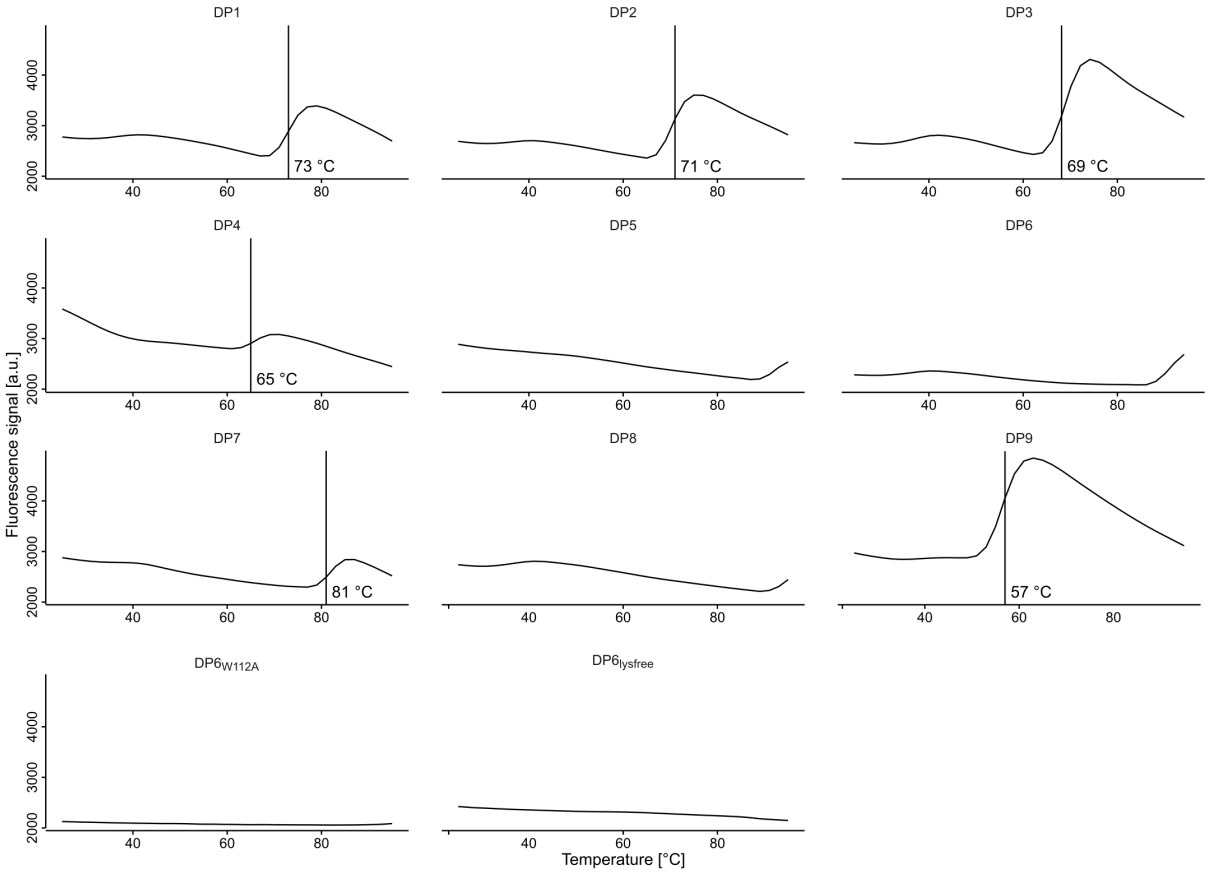

Supplementary Fig. S23. Differential scanning fluorimetry (thermofluor assay) of DARPins. *The fluorescence signal increase was measured as a function of temperature, based on the interaction of SYPRO Orange with hydrophobic regions becoming accessible through partial unfolding. Vertical lines indicate regions where the highest fluorescence signal change per temperature change was observed.*

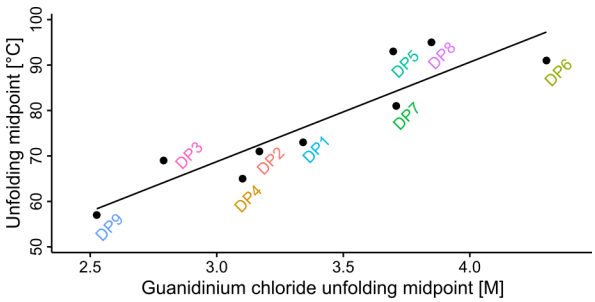

Supplementary Fig. S24. Comparison of structural stability of DARPins, derived from denaturant-induced equilibrium unfolding measured by circular dichroism with the thermofluor assay.

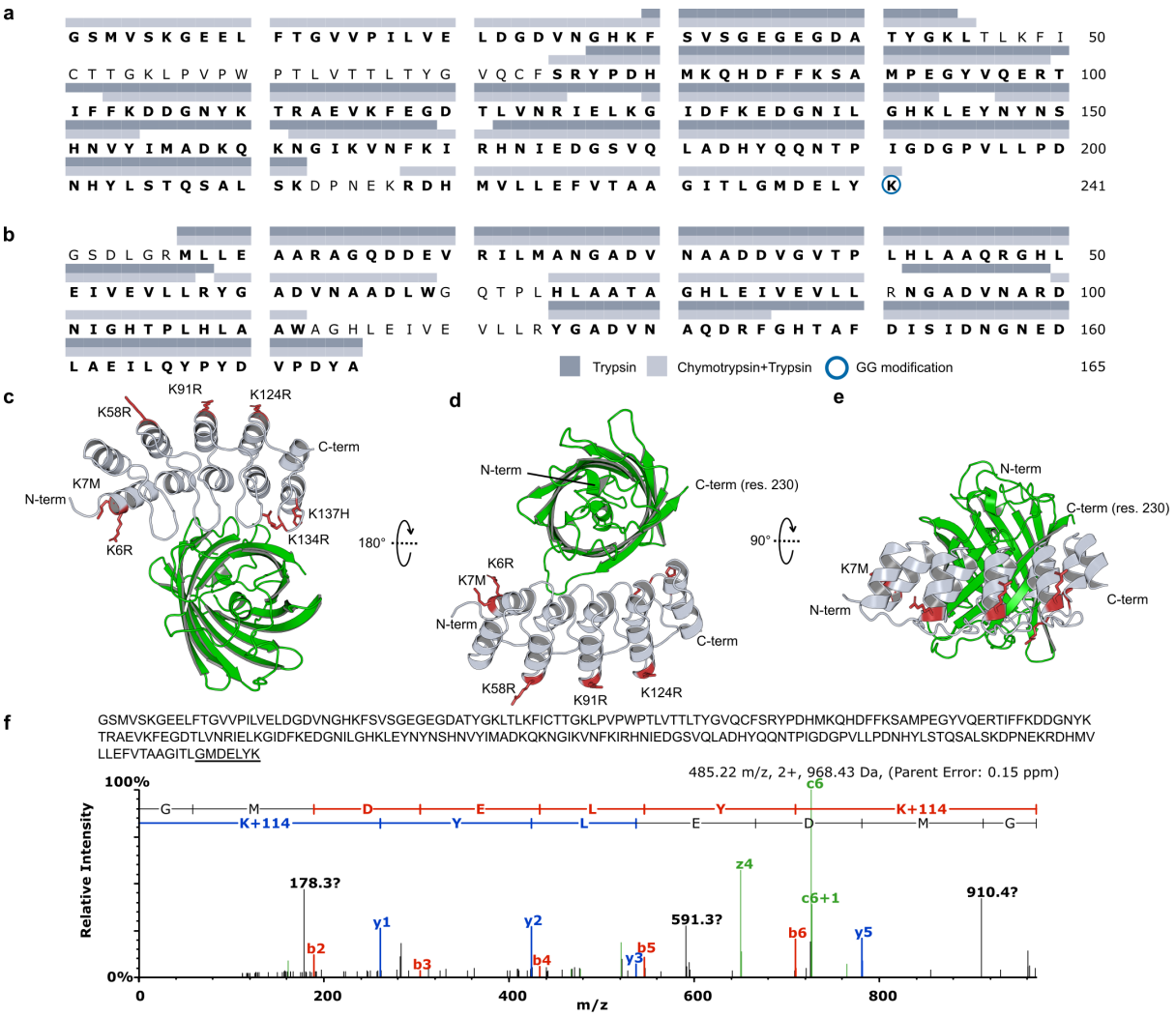

Supplementary Fig. S25. DP6$_{lysfree}$ ubiquitination sites found after pulldown of HA-tagged DP6$_{lysfree}$ in complex with GS-eGFP from HEK293 lysate ubiquitination assay and subsequent MS-MS analysis. a-b, *Sequence coverage and modifications found in GS-eGFP (a) and DP6$_{lysfree}$-HA, with the tag being used for pulldown (b). The ubiquitinated lysine on GS-eGFP carries a covalent GG adduct.* ***c-e,*** *Crystal structure of DP6 with substituted amino acids according to mutated lysines (grey) in complex with eGFP (green). PDB ID 5MA6. The ubiquitination site on GS-eGFP K241 is not resolved in the structure. Lysine mutations in DP6 to produce DP6$_{lysfree}$ are shown in red. The M7K mutation in DP6$_{lysfree}$ lowers the complex degradation rate, and thus M7 in DP6$_{lysfree}$ likely represents a degron.* ***c,*** *Bottom view.* ***d,*** *Top view.* ***e,*** *Side view.* ***f,*** *Annotated tandem mass spectrum of ubiquitinated GS-eGFP peptide from pulldown of HEK293 lysate ubiquitination assay is shown with full amino acid sequence. MS-covered regions are underlined. Spectra are shown using the program Scaffold viewer. Y-ion-fragments are colored blue and b-ion-fragments are colored red, and c and z-ion-fragments are colored green. Detected fragments are matched with positions of peptide bond breaks (vertical lines) within the displayed sequence (y-ion-fragments, lower sequence C-N-term orientation; b-ion-fragments, upper sequence N-C-term orientation). Within the sequence, amino acids and bonds are colored, if at least one consecutive fragment was found.*

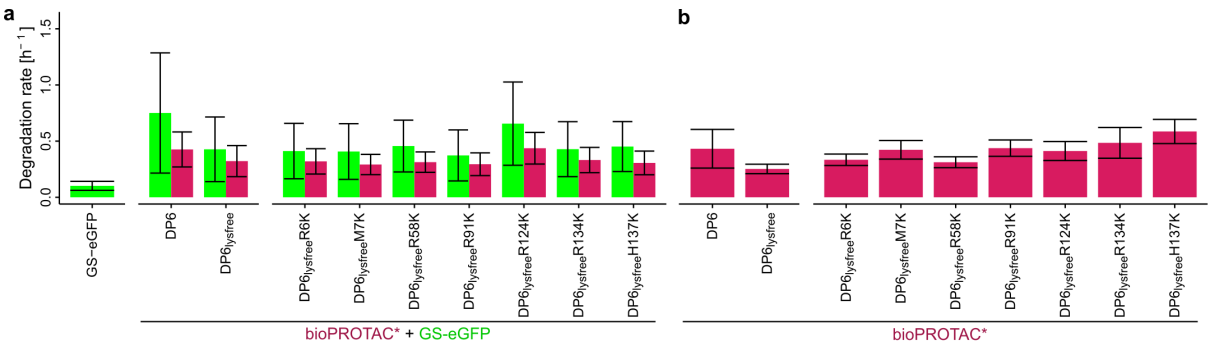

Supplementary Fig. S26. Degradation rates of bioPROTACs containing DP6$_{lysfree}$ and single lysine back-mutations in complex with eGFP (a) or alone (b). *GS-eGFP degradation rates are shown in green and degradation rates of bioPROTACs, labelled with TMR5-maleimide are shown in red. Shown are average degradation rate constants of single cells as determined after microinjection of one-to-one complexes or bioPROTACS by themselves into the cytosol of living cells observed by fluorescent live-cell imaging. Error bars indicate standard deviations. Numbers of analyzed cells per analyte are shown in Supplementary Table ST2.*

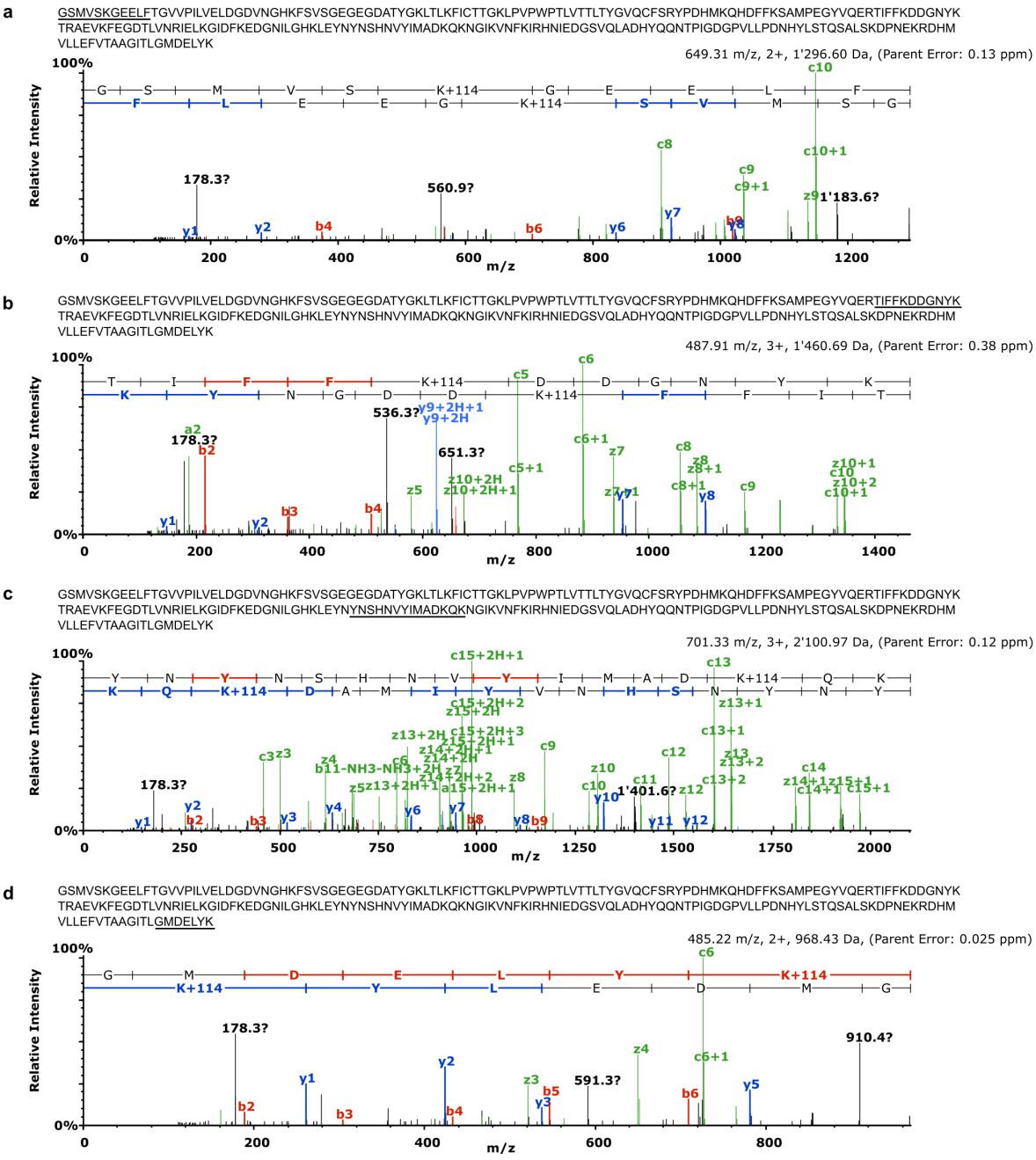

Supplementary Fig. S27. GS-eGFP ubiquitination sites observed after interaction with DP6-bioPROTAC. *Sequence coverage and modification sites are shown in Fig. 3a in the main manuscript. Here, select annotated tandem mass spectra of ubiquitinated GS-eGFP peptides from CHIP in-vitro ubiquitination assay are shown with full amino acid sequences to show ubiquitination of GS-eGFP by DP6-bioPROTAC on four lysines. MS-covered regions are underlined. Spectra are shown using the program Scaffold viewer. Y-ion-fragments are colored blue, b-ion-fragments are colored red, and c and z-ion-fragments are colored green. Detected fragments are matched with positions of peptide bond breaks (vertical lines) within the displayed sequence (y-ion-fragments, lower sequence C-N-term orientation; b-ion-fragments, upper sequence N-C-term orientation). Within the sequence, amino acids and bonds are colored if at least one consecutive fragment was found.* ***a****, K6.* ***b****, K104.* ***c****, K159.* ***d****, K241.*

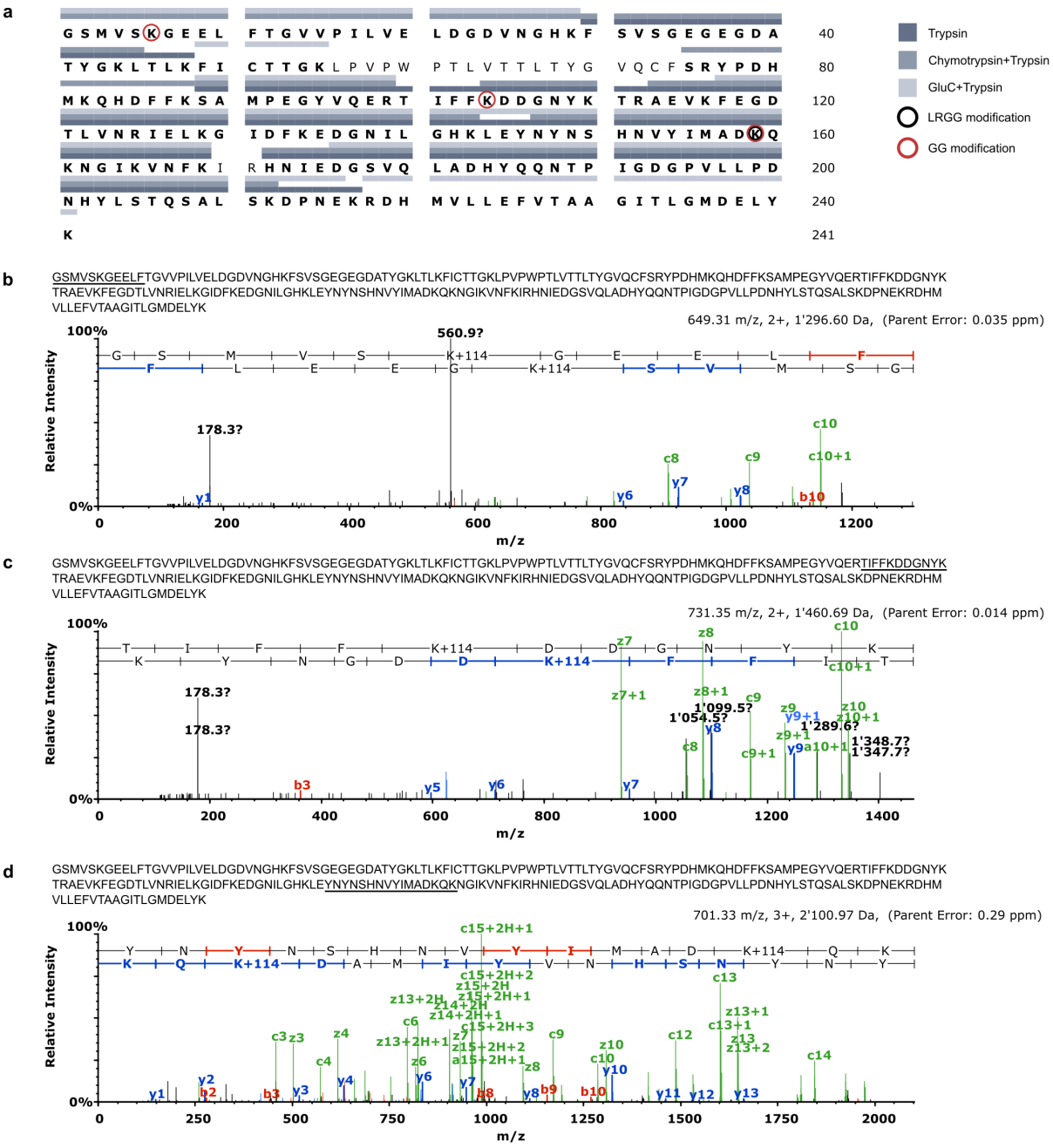

Supplementary Fig. S28. GS-eGFP ubiquitination sites observed after interaction with DP7-bioPROTAC. ***a****, Sequence coverage and modifications found in GS-eGFP.* ***b-d****, Select annotated tandem mass spectra of ubiquitinated GS-eGFP peptides from an in-vitro ubiquitination assay are shown with full amino acid sequences to show ubiquitination of GS-eGFP by DP7-bioPROTAC on three lysines. MS-covered regions are underlined. Spectra are shown using the program Scaffold viewer. Y-ion-fragments are colored blue, b-ion-fragments are colored red, and c and z-ion-fragments are colored green. Detected fragments are matched with positions of peptide bond breaks (vertical lines) within the displayed sequence (y-ion-fragments, lower sequence C-N-term orientation; b-ion-fragments, upper sequence N-C-term orientation). Within the sequence, amino acids and bonds are colored if at least one consecutive fragment was found.* ***b****, K6.* ***c****, K104.* ***d****, K159.*

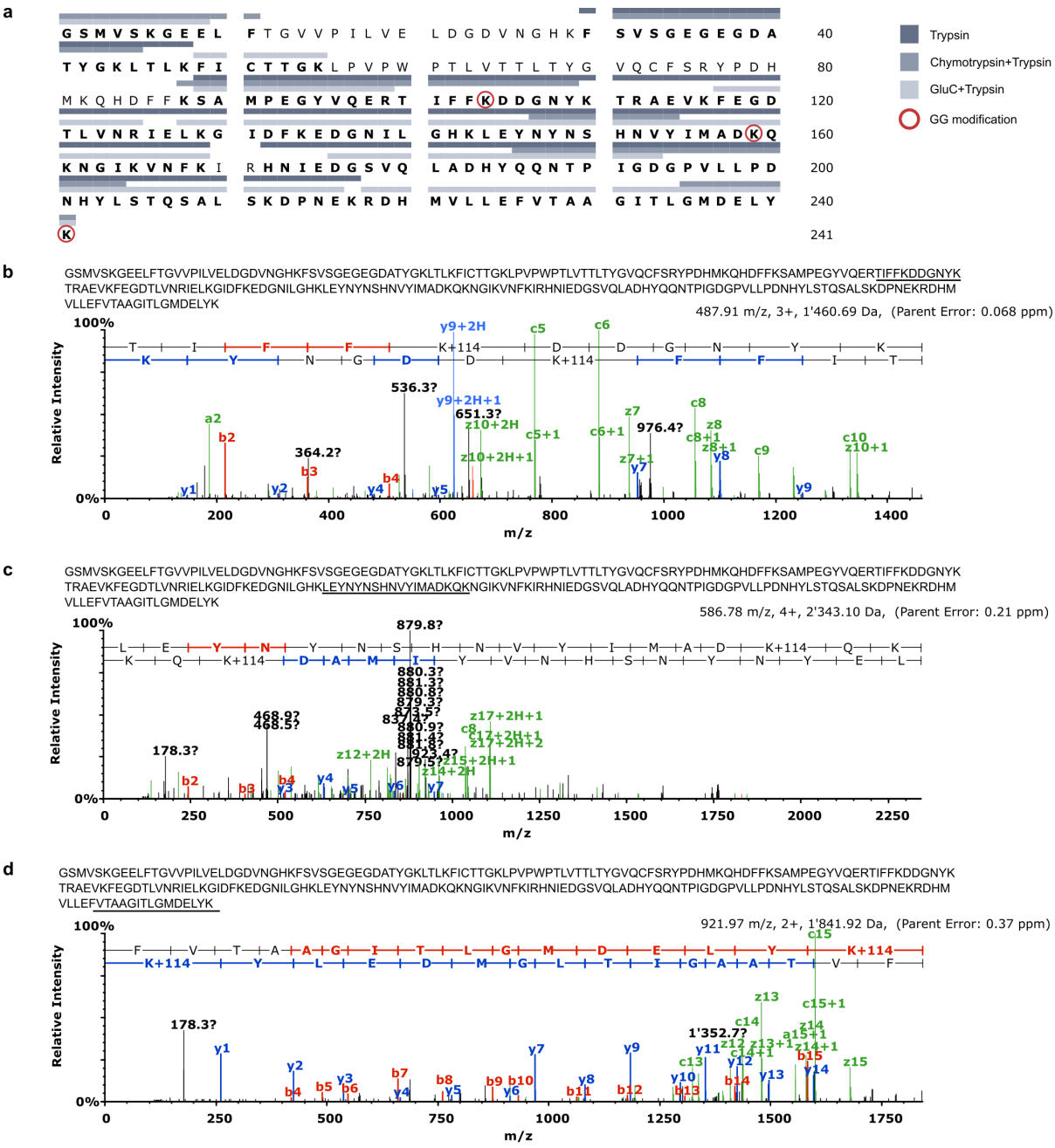

Supplementary Fig. S29. GS-eGFP ubiquitination sites observed after interaction with DP9-bioPROTAC. ***a****, Sequence coverage and modifications found in GS-eGFP.* ***b-d****, Select annotated tandem mass spectra of ubiquitinated GS-eGFP peptides from CHIP in-vitro ubiquitination assay are shown with full amino acid sequences to show ubiquitination of GS-eGFP by DP9-bioPROTAC on three lysines. MS-covered regions are underlined. Spectra are shown using the program Scaffold viewer. Y-ion-fragments are colored blue, b-ion-fragments are colored red, and c and z-ion-fragments are colored green. Detected fragments are matched with positions of peptide bond breaks (vertical lines) within the displayed sequence (y-ion-fragments, lower sequence C-N-term orientation; b-ion-fragments, upper sequence N-C-term orientation). Within the sequence, amino acids and bonds are colored if at least one consecutive fragment was found.* ***b****, K104.* ***c****, K159.* ***d****, K241.*

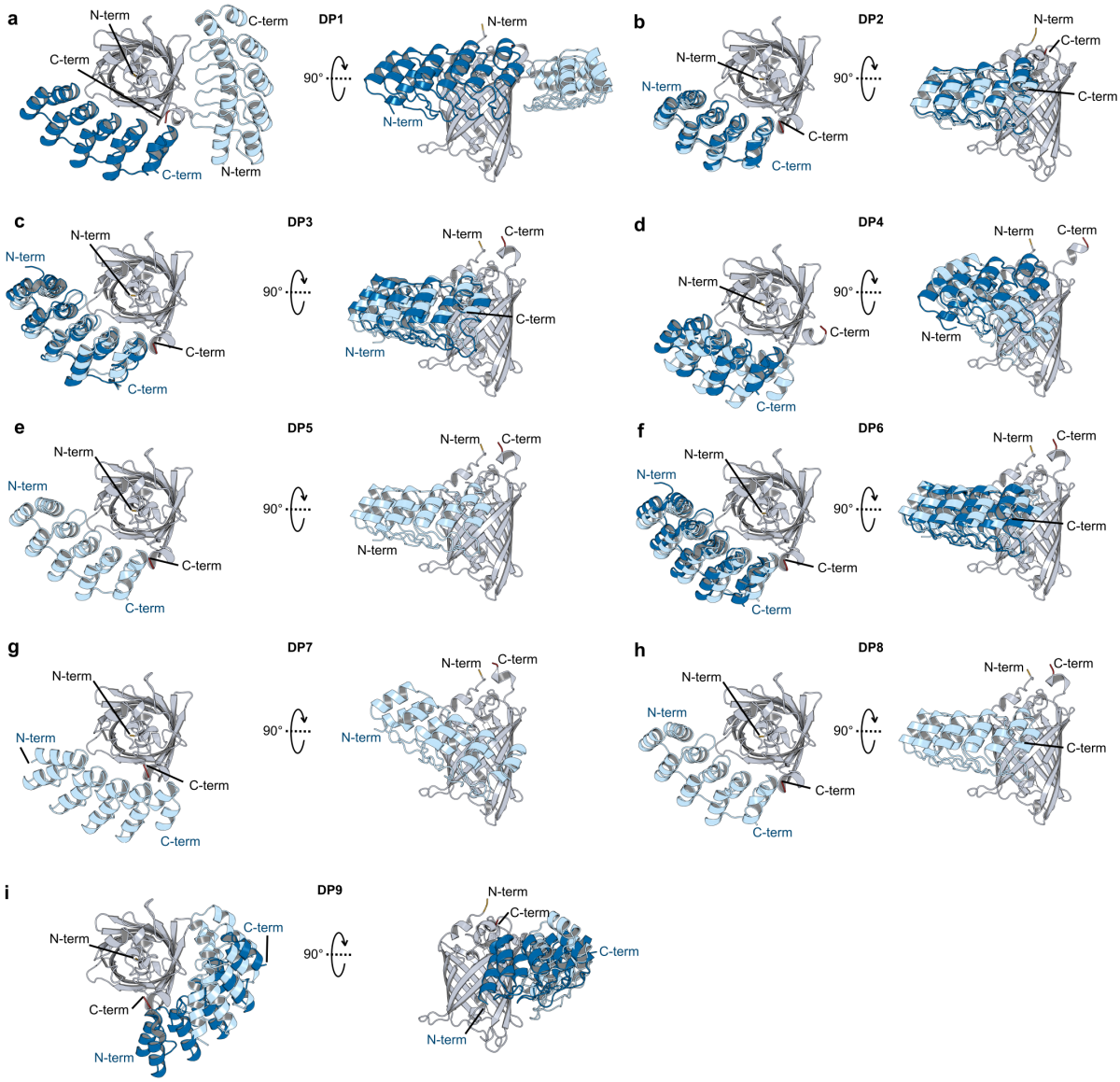

Supplementary Fig. S30. Structural representations of DARPin/eGFP complexes*. Structures of DARPin/eGFP complexes were created in PyMOL. The DARPins from DARPin/eGFP complex structures determined by X-ray crystallography are colored dark blue. Models created by AlphaFold Multimer are shown for all complexes, including those determined by X-ray crystallography, with the DARPin colored in light blue. The prediction with the best interface Predicted Template Modeling Score (ipTM score) is always shown. All complexes were aligned on GFP (grey). The missing DARPins DP5 and DP8 differ only minimally from each other in sequence and from the solved complexes of DP6 and DP3, respectively (Fig. 1b), and are therefore expected to have a similar binding site on GFP, and this is also found in the AlphaFold Multimer predictions. Since the DP7 sequence does not have a close homolog, it was modeled both using AlphaFold Multimer and ColabDock (see Methods), both resulting in a pose similar to DP6, consistent with epitope binning (Supplementary Fig. S31).* ***a****, Structure of DP1 in complex with eGFP (PDB ID 9F22).* ***b****, Structure of DP2 in complex with eGFP (PDB ID 9F23).* ***c****, Structure of DP3 in complex with eGFP (PDB ID 6MWQ).* ***d****, Structure of DP4 in complex with eGFP (PDB ID 9F24).* ***e****, Structure of DP5 in complex with eGFP (similar in sequence to DP6, AlphaFold model).* ***f****, Structure of DP6 in complex with eGFP (PDB ID 5MA6).* ***g****, Structure of DP7 in complex with eGFP, AlphaFold model, see Methods).* ***h****, Structure of DP8 in complex with eGFP (similar in sequence to DP6, AlphaFold model).* ***i****, Structure of DP9 in complex with eGFP (PDB ID 5MAD).*

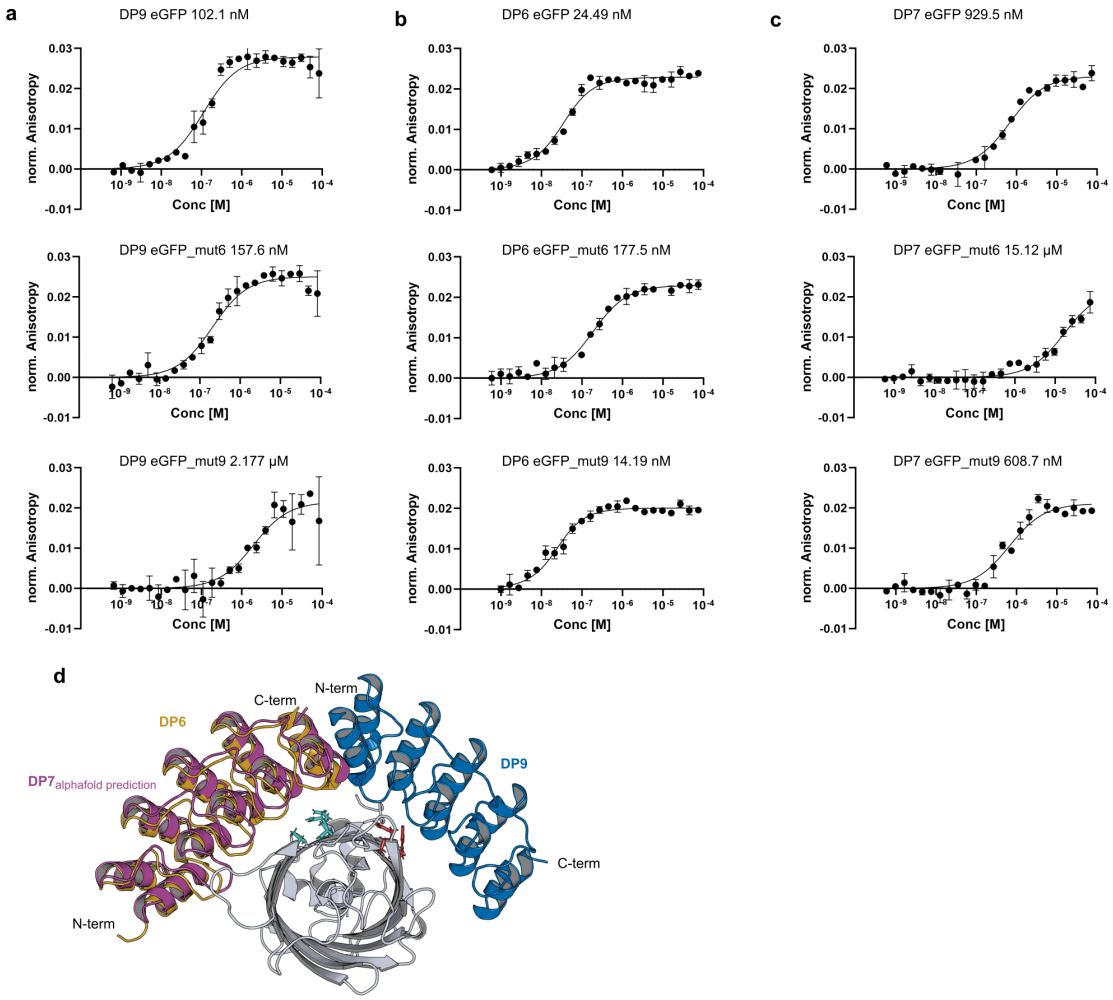

Supplementary Fig. S31. GS-eGFP epitope binning experiments with DARPins by fluorescence anisotropy to determine the epitope of DP7. *eGFP mutants were produced that were expected from the molecular structures to hinder binding of either DP6 (eGFP_Q207A_A209Y (cyan): termed eGFP_mut6) or DP9 (eGFP_Y154A_R171A (red): termed eGFP_mut9) (see structure in (d)). These mutations were derived from Rosetta energy calculations, resulting in the energies for DARPin mutant interactions with eGFP in the complex structures: DP9/eGFP: -22.6 REU, DP9/eGFP_mut9: ca. -16 REU. DP6/eGFP: -23.3 REU, DP6/eGFP_mut6: -14.8 REU.* ***a-c,*** *Fluorescence anisotropy titrations: wt-eGFP (top), eGFP mut6 (middle), eGFP mut9 (bottom).* ***a,*** *Affinity determinations of DP9 with eGFP variants.* ***b,*** *Affinity determinations of DP6 with eGFP variants.* ***c,*** *Affinity determinations of DP7 with GS-eGFP variants.* ***d,*** *Crystal structure of eGFP (gray) bound to DP6 (yellow) and DP9 (blue). Mutations on eGFP to reduce affinity of either of the DARPins are shown as sticks. Mutations to produce the eGFP_mut6 (eGFP_Q207A_A209Y) variant are shown in cyan, mutations for eGFP_mut9 (eGFP_Y154A_R171A) are shown in red. The GS-GFP_mut6 set reduces affinity of DP7. DP7 binding epitope most likely overlaps with that of DP6.*

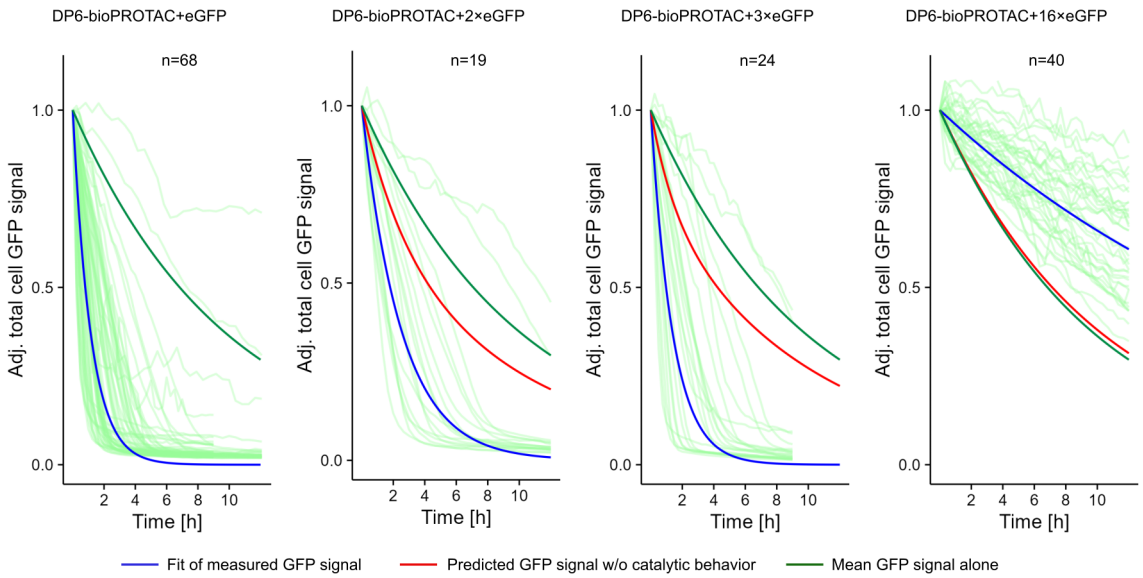

Supplementary Fig. S32. DP6-bioPROTAC is able to degrade GS-eGFP catalytically. *Shown are single cell fluorescence curves of HEK293 cells injected with DP6-bioPROTAC/GS-eGFP complexes in different stoichiometric ratios, with identical DP6-bioPROTAC concentration and increasing amounts of substrate GS-eGFP. Thin green lines are single-cell GS-eGFP fluorescence traces. The thick green line (identical in all panels) is the averaged curve of GS-eGFP alone, obtained in independent traces, not shown here. The blue line is the averaged actually measured curve in the various panels. The red curve assumes the absence of catalytic turnover, and thus that DP6-bioPROTAC would degrade one equivalent of GS-eGFP with a fast rate and then the remaining GS-eGFP is degraded with its slow intrinsic rate. The observed rate, however, is faster than this predicted rate up to a 3-fold excess of GS-eGFP. It is currently unclear why the observed rate becomes very slow at very high GS-eGFP concentrations, possibly since also the DP6-bioPROTAC-independent degradation becomes saturated.*

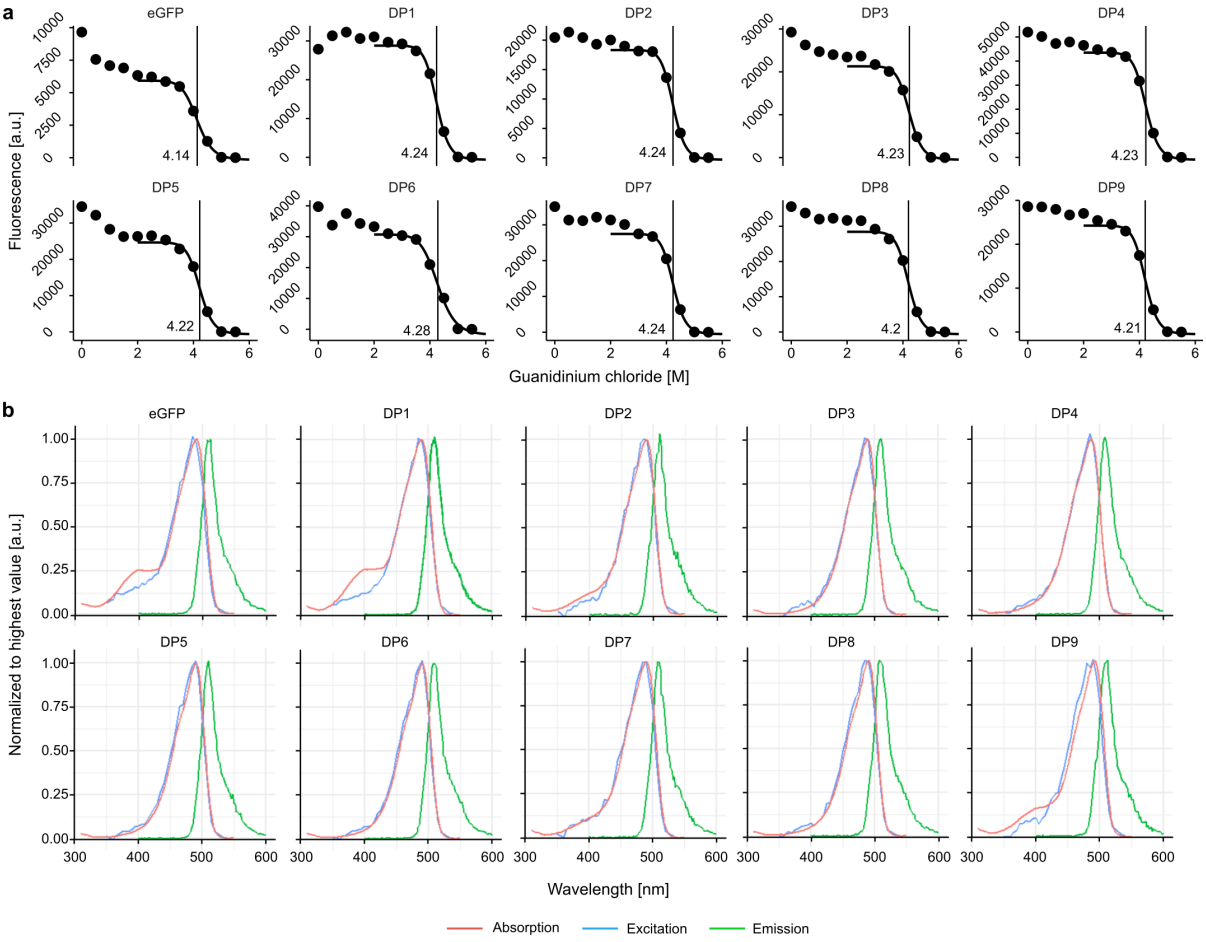

Supplementary Fig. S33. DARPin-binding does not influence GS-eGFP structural stability but can have an impact on GS-eGFP absorption. a, *GS-eGFP fluorescence as a function of guanidinium chloride concentration for GS-eGFP alone or GS-eGFP in complex with the indicated DARPin.* ***b,*** *Changes in GS-eGFP fluorescence based on interaction with different DARPins. Fluorescence emission signals (green) were recorded after excitation at 490 nm. This wavelength represents the main absorption peak of GS-eGFP (red). Excitation curves (blue) represent the fluorescence intensity recorded at 520 nm as a function of changed excitation wavelength. Signals are normalized to the highest peak. It is of note that the shape of emission spectra (green) is identical for all complexes and GS-eGFP alone. As expected for GS-eGFP alone, we see two absorption peaks at 400 and 480 nm, with the 400 nm peak constituting a shoulder to the left. Interaction with certain DARPins leads to reduced absorption and excitation at 400 nm, which indicates the absence of GS-eGFP in the protonated state[1]. This suggests that the binding of some DARPins induces a slight structural modification in the vicinity of the chromophore cavity. Given the minute amounts of structural changes leading to such spectral changes, and their internal location within the chromophore cavity, we are confident that neither stability nor degradation rates are influenced. Other proteins binding to GFP, such as some nanobodies, have also shown this behavior.[2]*

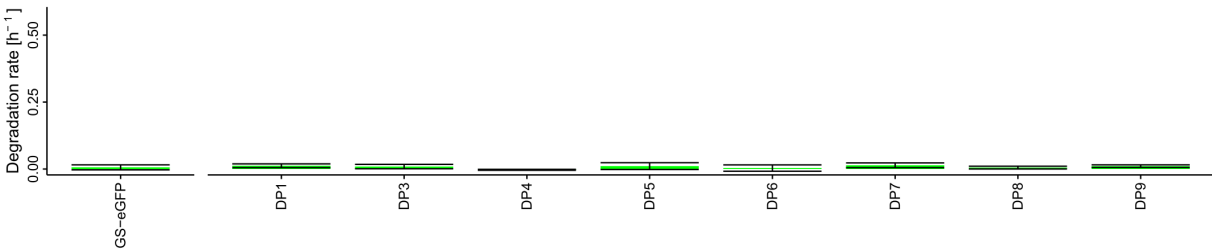

Supplementary Fig. S34. Degradation rates of DARPin/GS-eGFP complexes with 10 µM proteasome inhibitor MG132. *Shown are average degradation rate constants of single cells as determined after microinjection of one-to-one complexes into the cytosol of living cells observed by fluorescent live-cell imaging. Error bars indicate standard deviations.* *Numbers of analyzed cells per analyte are shown in Supplementary Table ST2.*

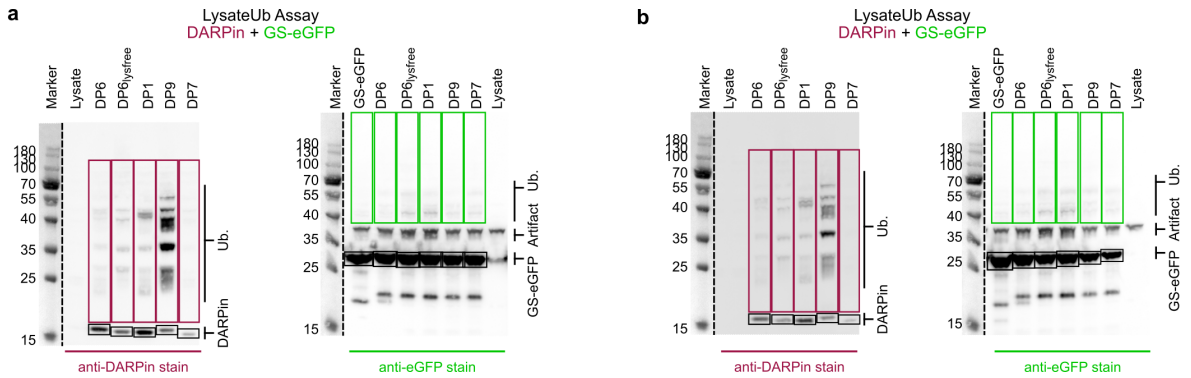

Supplementary Fig. S35. Replicates of LysateUb assay of various DARPin/GS-eGFP complexes of Fig. 3h. *Total number of replicates of this assay was n=3 for the quantification of ubiquitination. Samples were split for staining with anti-eGFP antibody or anti DARPin serum to detect GS-eGFP or DARPin ubiquitination. Unedited blots can be seen in Fig. S16.*

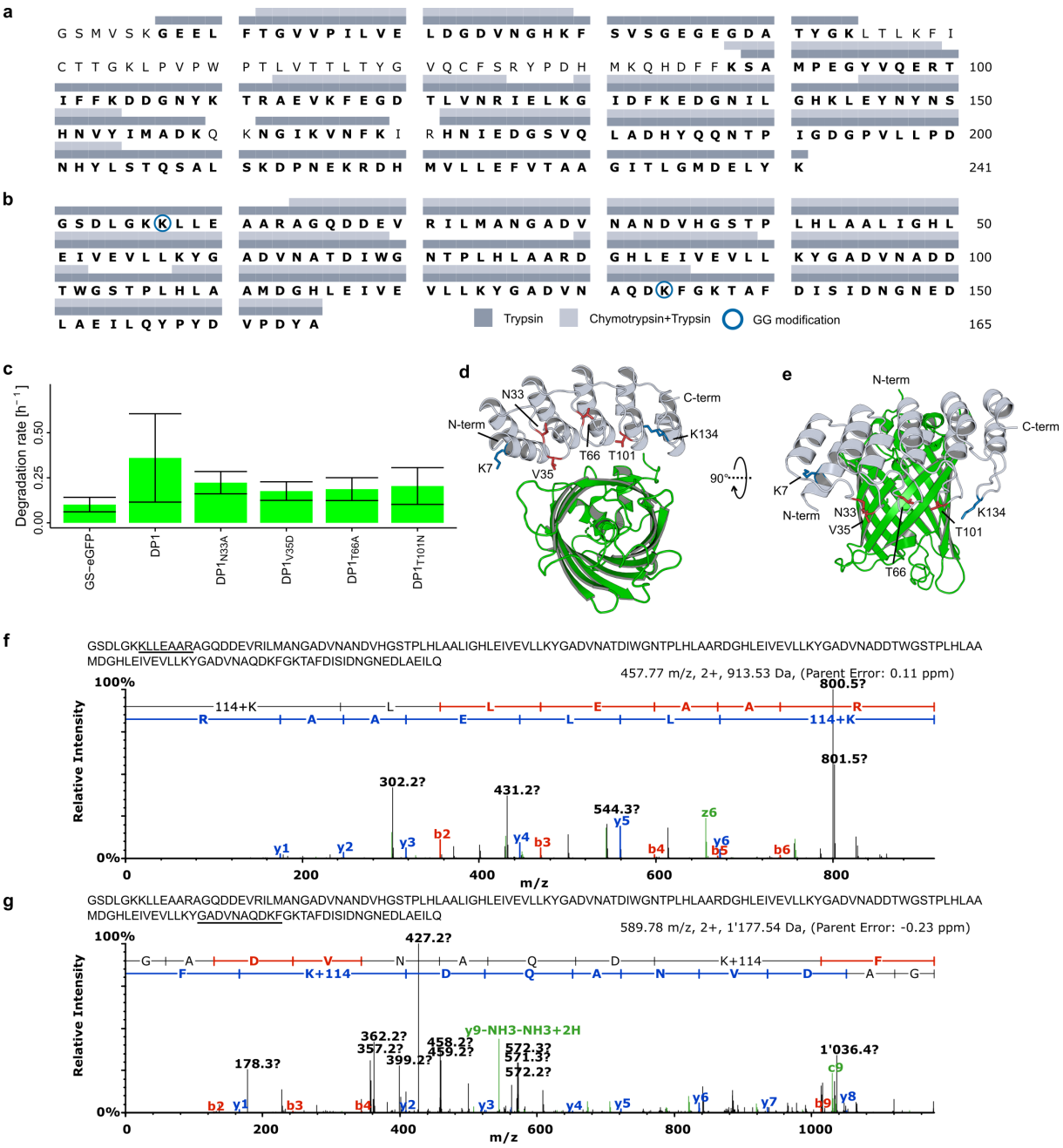

Supplementary Fig. S36. DP1 ubiquitination sites found after pulldown of HA-tagged DP1 in complex with GS-eGFP from HEK293 lysate ubiquitination assay and subsequent MS-MS analysis. *Ubiquitinated lysines carry a GG covalent adduct.* ***a-b****, Sequence coverage and modifications found in GS-eGFP (a) and DP1-HA, with the tag being used for pulldown (b).* ***c****, Degradation rates of GS-eGFP in complex with DP1 mutants. Four amino acids unique to DP1 were mutated to determine if they constitute a degron. Shown are average degradation rate constants of single cells as determined after microinjection of one-to-one complexes into the cytosol of living cells observed by fluorescence live-cell imaging. Error bars indicate standard deviations. Numbers of analyzed cells per analyte are shown in Supplementary Table ST2.* ***d-e****, Crystal structure of DP1 (grey) in complex with eGFP (green), PDB ID 9F22. Mutations introduced into DP1 to determine potential degrons are shown in red. Ubiquitination sites K7 and K134, determined by ubiquitination assays in HEK293 lysate and subsequent MS-MS analysis are shown in blue.* ***d****, top view.* ***e****, side view.* ***f-g****, Annotated tandem mass spectra of ubiquitinated DARPin peptides from pulldown of ubiquitination assays in HEK293 lysate are shown with full amino acid sequences. MS-covered regions are underlined. Spectra are shown using the program Scaffold viewer. Y-ion-fragments are colored blue and b-ion-fragments are colored red, and c and z-ion-fragments are colored green. Detected fragments are matched with positions of peptide bond breaks (vertical lines) within the displayed sequence (y-ion-fragments, lower sequence C-N-term orientation; b-ion-fragments, upper sequence N-C-term orientation). Within the sequence, amino acids and bonds are colored if at least one consecutive fragment was found.* ***f****, K7.* ***g****, K134.*

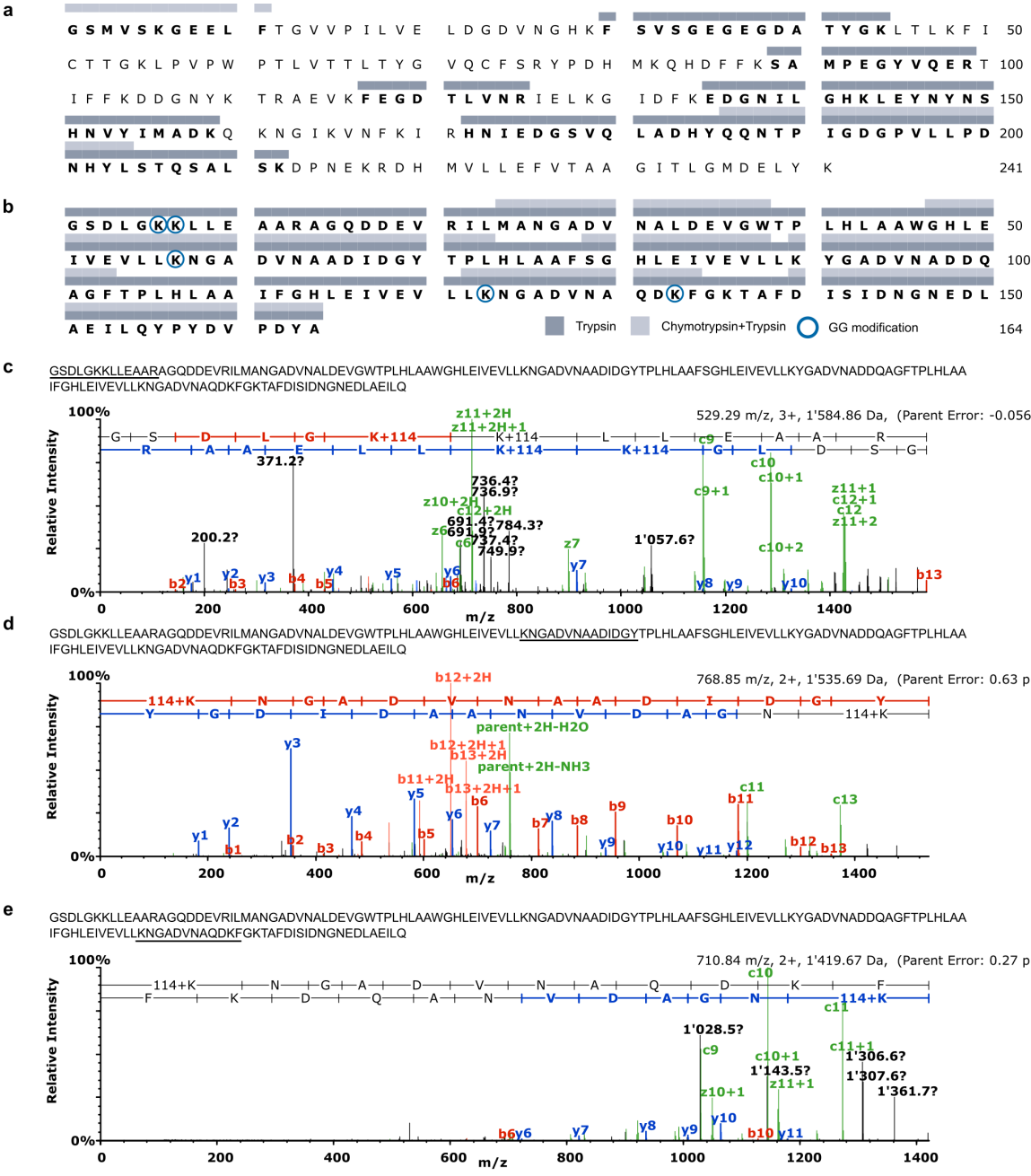
a
GSMVSKGEEL FTGVVPILVE LDGDVNGHKF SVSGEGEGDA TYGKLTLKFI 50
CTTGKLPVPW PTLVTTLTYG VQCFSRYPDH MKQHDFFKSA MPEGYVQERT 100
IFFKDDGNYK TRAEVKFEGD TLVNRIELKG IDFKEDGNIL GHKLEYNYNS 150
HNVYIMADKQ KNGIKVNFKI RHNIEDGSVQ LADHYQQNTP IGDGPVLLPD 200
NHYLSTQSAL SKDPNEKRDH MVLLEFVTAA GITLGMDELY K 241
b
GSDLGKKLLE AARAGQDDEV RILMANGADV NALDEVGWTP LHLAAWGHLE 50
IVEVLLKNGA DVNAADIDGY TPLHLAAFSG HLEIVEVLLK YGADVNADDQ 100
AGFTPLHLAA IFGHLEIVEV LLKNGADVNA QDKFGKTAFD ISIDNGNEDL 150
AEILQYPYDV PDYA 164
Trypsin
Chymotrypsin+Trypsin
GG modification
c
GSDLGKKLLEAARAGQDDEVRILMANGADVNALDEVGWTPLHLAAWGHLEIVEVLLKNGADVNAADIDGYTPLHLAAFSGHLEIVEVLLKYGADVNADDQAGFTPLHLAA
IFGHLEIVEVLLKNGADVNAQDKFGKTAFDISIDNGNEDLAEILQ
529.29 m/z, 3+, 1'584.86 Da, (Parent Error: -0.056 ppm)
Relative Intensity
m/z
d
GSDLGKKLLEAARAGQDDEVRILMANGADVNALDEVGWTPLHLAAWGHLEIVEVLLKNGADVNAADIDGYTPLHLAAFSGHLEIVEVLLKYGADVNADDQAGFTPLHLAA
IFGHLEIVEVLLKNGADVNAQDKFGKTAFDISIDNGNEDLAEILQ
768.85 m/z, 2+, 1'535.69 Da, (Parent Error: 0.63 ppm)
Relative Intensity
m/z
e
GSDLGKKLLEAARAGQDDEVRILMANGADVNALDEVGWTPLHLAAWGHLEIVEVLLKNGADVNAADIDGYTPLHLAAFSGHLEIVEVLLKYGADVNADDQAGFTPLHLAA
IFGHLEIVEVLLKNGADVNAQDKFGKTAFDISIDNGNEDLAEILQ
710.84 m/z, 2+, 1'419.67 Da, (Parent Error: 0.27 ppm)
Relative Intensity
m/z

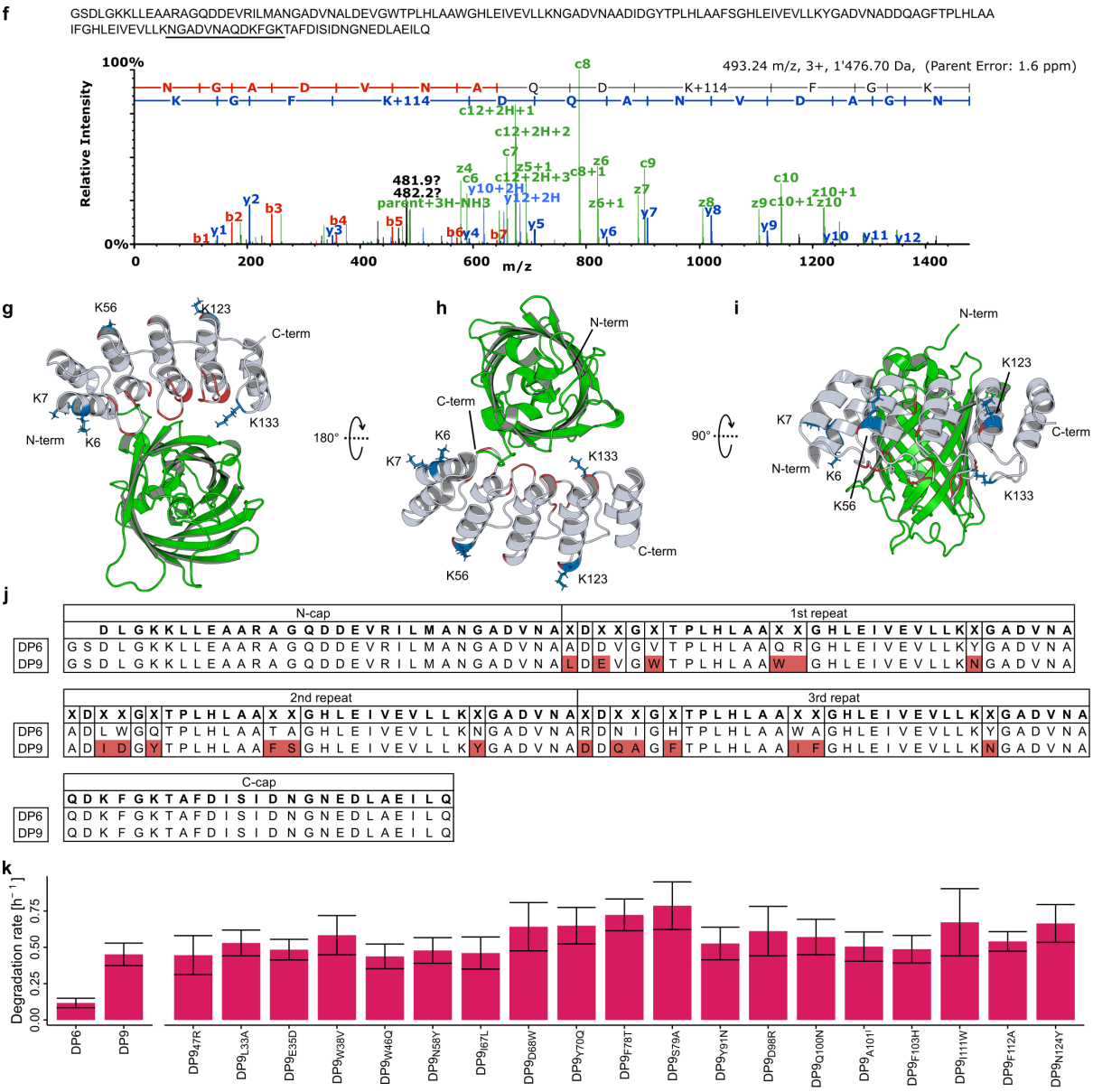

Supplementary Fig. S37. DP9 ubiquitination sites found after pulldown of HA-tagged DP9 in complex with GS-eGFP from HEK293 lysate ubiquitination assay and subsequent MS-MS analysis. a-b*, Sequence coverage and modifications found in GS-eGFP (a) and DP9-HA (b). Ubiquitinated lysines carry a covalent GG adduct.* ***c-f****, Annotated tandem mass spectrum of ubiquitinated DARPin peptides from pulldown ubiquitination assays in HEK293 lysate are shown with full amino acid sequence. MS-covered regions are underlined. Spectra are shown using the program Scaffold viewer. Y-ion-fragments are colored blue and b-ion-fragments are colored red, and c and z-ion-fragments are colored green. Detected fragments are matched with positions of peptide bond breaks (vertical lines) within the displayed sequence (y-ion-fragments, lower sequence C-N-term orientation; b-ion-fragments, upper sequence N-C-term orientation). Within the sequence, amino acids and bonds are colored if at least one consecutive fragment was found.* ***c****, K6 and K7.* ***d****, K56.* ***e****, K123.* ***f****, K133.* ***g-i****, Crystal structure of DP6 (grey) in complex with eGFP (green), PDB ID 5MAD. Ubiquitinated lysines in DP9 are shown in blue. Amino acids in DP9 differing from DP6 that were mutated to find potential degrons are shown in red. None of the residues constitute a degron on its own.* ***g****, bottom view.* ***h****, top view.* ***i****, side view.* ***j****, Sequence alignment of DP6, DP9. Amino acids differing in DP9 from DP6 that were mutated to find potential degrons are colored red.* ***k****, Degradation rates of labelled DP6, DP9 and DP9 mutants as shown in j. Shown are average degradation rate constants of single cells as determined after microinjection of into the cytosol of living cells observed by fluorescence live-cell imaging. Error bars indicate standard deviations. Numbers of analyzed cells per analyte are shown in Supplementary Table ST2.*

Supplementary Tables

Supplementary Table ST1: Number of analyzed cells of eGFP channel (n_{GFP}) or dye channel (n_{dye}) of unique analytes (* denotes dye label), bar graphs of which are shown in Figures 2-4.

Fig. 2a-b			Fig. 3d			Fig. 4a-c			Fig. 4k-o		
Analyte	**n_{GFP}**	**n_{dye}**	**Analyte**	**n_{GFP}**	**n_{dye}**	**Analyte**	**n_{GFP}**	**n_{dye}**	**Analyte**	**n_{GFP}**	**n_{dye}**
GS-eGFP	4046	-	GS-eGFP+DP6-bioPROTAC	66	-	DP1+GS-eGFP	15	-	DP6_lysfree_R6K*	-	50
DP1-bioPROTAC* +GS-eGFP	35	35	GS-eGFP_mut1	20	-	DP2+GS-eGFP	21	-	DP6_lysfree_M7K*	-	22
DP2-bioPROTAC* +GS-eGFP	34	35	GS-eGFP_mut1 +DP6-bioPROTAC	36	-	DP3+GS-eGFP	63	-	DP6_lysfree_R58K*	-	30
DP3-bioPROTAC* +GS-eGFP	26	25	GS-eGFP_mut1 +DP6-bioPROTAC_R272A	30	-	DP4+GS-eGFP	29	-	DP6_lysfree_R91K*	-	36
DP4-bioPROTAC* +GS-eGFP	21	21	GS-eGFP_mut2	25	-	DP5+GS-eGFP	35	-	DP6_lysfree_R124K*	-	36
DP5-bioPROTAC* +GS-eGFP	41	41	GS-eGFP_mut2 +DP6-bioPROTAC	34	-	DP6+GS-eGFP	103	-	DP6_lysfree_R134K*	-	42
DP6-bioPROTAC* +GS-eGFP	46	46	GS-eGFP_mut2 +DP6-bioPROTAC_R272A	25	-	DP7+GS-eGFP	62	-	DP6_lysfree_H137K*	-	67
DP7-bioPROTAC* +GS-eGFP	15	20	GS-eGFP_mut3	18	-	DP8+GS-eGFP	34	-	DP6_lysfree_R6K* +GS-eGFP	32	32
DP8-bioPROTAC* +GS-eGFP	32	33	GS-eGFP_mut3 +DP6-bioPROTAC	53	-	DP9+GS-eGFP	37	-	DP6_lysfree_M7K* +GS-eGFP	19	20
DP9-bioPROTAC* +GS-eGFP	36	35	GS-eGFP_mut3 +DP6-bioPROTAC_R272A	31	-	DP6_lysfree+GS-eGFP	197	-	DP6_lysfree_R58K* +GS-eGFP	23	25
DP6_W112A-bioPROTAC* +GS-eGFP	24	25	GS-eGFP_mut4	29	-	DP1*+GS-eGFP	37	36	DP6_lysfree_R91K* +GS-eGFP	30	30
DP6_dest-bioPROTAC* +GS-eGFP	53	55	GS-eGFP_mut4 +DP6-bioPROTAC	70	-	DP2*+GS-eGFP	23	22	DP6_lysfree_R124K* +GS-eGFP	32	34
DP6_lysfree-bioPROTAC* +GS-eGFP	23	23	GS-eGFP_mut4 +DP6-bioPROTAC_R272A	31	-	DP3*+GS-eGFP	39	39	DP6_lysfree_R134K* +GS-eGFP	34	34
DP6-bioPROTAC_R272A +GS-eGFP	24	-				DP4*+GS-eGFP	39	39	DP6_lysfree_H137K* +GS-eGFP	26	27
DP6-bioPROTAC* +GS-eGFP+MG132	28	27				DP5*+GS-eGFP	34	34	DP6_lysfree_R6K +GS-eGFP	40	-
GS-CHIP*	-	54				DP6*+GS-eGFP	36	37	DP6_lysfree_M7K +GS-eGFP	20	-
DP1-bioPROTAC*	-	35				DP7*+GS-eGFP	35	35	DP6_lysfree_R58K +GS-eGFP	43	-
DP2-bioPROTAC*	-	26				DP8*+GS-eGFP	31	30	DP6_lysfree_R91K +GS-eGFP	28	-
DP3-bioPROTAC*	-	27				DP9*+GS-eGFP	27	27	DP6_lysfree_R124K +GS-eGFP	32	-

DP4-bioPROTAC*	-	17
DP5-bioPROTAC*	-	25
DP6-bioPROTAC*	-	22
DP7-bioPROTAC*	-	35
DP8-bioPROTAC*	-	31
DP9-bioPROTAC*	-	32
DP6_W112A-bioPROTAC*	-	51
DP6_dest-bioPROTAC*	-	51
DP6_lysfree-bioPROTAC*	-	31
DP9_R47-bioPROTAC*	-	40
DP6-bioPROTAC* +MG132	-	29

DP6_W112A*+GS-eGFP	19	18
DP6_dest*+GS-eGFP	37	39
DP6_lysfree*+GS-eGFP	29	29
DP1*	-	24
DP2*	-	31
DP3*	-	31
DP4*	-	26
DP5*	-	40
DP6*	-	37
DP7*	-	28
DP8*	-	33
DP9*	-	22
DP6_W112A*	-	22
DP6_dest*	-	32
DP6_lysfree*	-	32
DP947R*	-	43

DP6_lysfree_R134K +GS-eGFP	24	-
DP6_lysfree_H137K +GS-eGFP	21	-
acetDP6_lysfree +GS-eGFP	28	-
DP6+GS-eGFP +GS-eGFP_MG132	32	-
DP6_lysfree +GS-eGFP_MG132	45	-
acetDP6_lysfree +GS-eGFP_MG132	5	-
DP6+GS-eGFP_E1inh	14	-
DP6_lysfree +GS-eGFP_E1inh	14	-
DP1_lysfree +GS-eGFP	16	-
DP4_lysfree +GS-eGFP	30	-

Supplementary Table ST2: Number of analyzed cells with eGFP signal (n_{GFP}) or dye signal (n_{dye}) of unique analytes (* denotes dye label), bar graphs of which are shown in Supplementary Figures 1-37.

Supplementary Fig. S1a			Supplementary Fig. S26a-b			Supplementary Fig. S34			Supplementary Fig. S36c			Supplementary Fig. S37k		
Analyte	**n_{GFP}**	**n_{dye}**	**Analyte**	**n_{GFP}**	**n_{dye}**	**Analyte**	**n_{GFP}**	**n_{dye}**	**Analyte**	**n_{GFP}**	**n_{dye}**	**Analyte**	**n_{GFP}**	**n_{dye}**
DP6bio_ PROTAC_ C181A +GS-eGFP	22	-	DP6_lysfree_ R6K_bio_ PROTAC* +GS-eGFP	35	37	GS-eGFP +MG132	160	-	DP1_N33A	32	-	DP9_L33A*	-	39
DP6bio_ PROTAC_ C200A +GS-eGFP	15	-	DP6_lysfree_ M7K_ bioPROTAC* +GS-eGFP	27	27	DP1+GS-eGFP +MG132	4	-	DP1_V35D	31	-	DP9_E35D*	-	43
DP6bio_ PROTAC_ C181A_ C200A +GS-eGFP	28	-	DP6_lysfree_ R58K_ bioPROTAC* +GS-eGFP	29	29	DP3+GS-eGFP +MG132	13	-	DP1_T66A	35	-	DP9_W38V*	-	61
			DP6_lysfree_ R91K_ bioPROTAC* +GS-eGFP	16	15	DP4+GS-eGFP +MG132	3	-	DP1_T101N	32	-	DP9_W46Q*	-	67
			DP6_lysfree_ R124K_ bioPROTAC* +GS-eGFP	22	23	DP5+GS-eGFP +MG132	6	-				DP9_N58Y*	-	40
			DP6_lysfree_ R134K_ bioPROTAC* +GS-eGFP	10	11	DP7+GS-eGFP +MG132	7	-				DP9_I67L*	-	32
			DP6_lysfree_ H137_ bioPROTAC* +GS-eGFP	17	17	DP8+GS-eGFP +MG132	12	-				DP9_D68W*	-	42
			DP6_lysfree_ R6K_ bioPROTAC*	-	26	DP9+GS-eGFP +MG132	6	-				DP9_Y70Q*	-	60
			DP6_lysfree_ M7K_ bioPROTAC*	-	34							DP9_F78T*	-	55
			DP6_lysfree_ R58K_ bioPROTAC*	-	19							DP9_S79A*	-	68
			DP6_lysfree_ R91K_ bioPROTAC*	-	32							DP9_Y91N*	-	30
			DP6_lysfree_ R124_ bioPROTAC*	-	28							DP9_D98R*	-	35
			DP6_lysfree_ R134_ bioPROTAC*	-	25							DP9_Q100N*	-	38

DP6_lysfree_H137_bioPROTAC*	-	32			DP9_A101I*	-	51
					DP9_F103H*	-	36
					DP9_I111W*	-	28
					DP9_F112A*	-	37
					DP9_N124Y*	-	28

References

1. Ehrig T., O'Kane D. J. & Prendergast F. G. Green-fluorescent protein mutants with altered fluorescence excitation spectra. *FEBS Lett.* **367**, 163-166 (1995).
2. Kirchhofer A. *et al.* Modulation of protein properties in living cells using nanobodies. *Nat. Struct. Mol. Biol.* **17**, 133-138 (2010).